

## Modeling streamflow dynamics under climate and land use shifts using MIKE SHE in the upper Omo Gibe catchment, Ethiopia

Kindie Zewdie Werede<sup>1</sup>, Tarun Kumar Lohani<sup>2+</sup>, Bogale Gebremariam Neka<sup>3</sup>, Getachew Bereta Geremew<sup>4</sup>

<sup>1</sup> PhD scholar in Hydraulic Engineering, Faculty of Hydraulic and Water Resources Engineering, Water Technology Institute, Arba Minch University, Arba Minch, Ethiopia

<sup>2</sup> Professor, Faculty of Hydraulic and Water Resources Engineering, Water Technology Institute, Arba Minch University, Arba Minch, Ethiopia

<sup>3</sup> Associate Professor, Faculty of Hydraulic and Water Resources Engineering, Water Technology Institute, Arba Minch University, Arba Minch, Ethiopia

<sup>4</sup> Associate Professor, Faculty of Hydraulic and Water Resources Engineering, Water Technology Institute, Arba Minch University, Arba Minch, Ethiopia

### Abstract

This study utilized the MIKE SHE hydrological model to analyze the combined effects of shifting climatic conditions and land use/land cover (LULC) changes on river discharge dynamics. We developed three distinct scenarios by integrating three climate data periods (1990–2000, 2001–2010, and 2011–2020) with three LULC maps (1990, 2005, and 2020). The model was systematically calibrated and validated, achieving strong performance metrics. The Nash-Sutcliffe Efficiency (NSE) and coefficient of determination ( $R^2$ ) were 0.83 and 0.82 for calibration, and 0.80 and 0.81 for validation, respectively, demonstrating the model's reliability in simulating the catchment's hydrological processes. Our findings reveal a substantial influence of both LULC and climate changes, with the most notable impacts observed during the 2001–2010 and 2011–2020 periods. LULC alterations increased surface runoff by 10.29% and 2.38%, while decreasing subsurface flow by 6.03% and 6.82%, and reducing evapotranspiration by 0.75% and 5.49%. Climate variations further amplified these effects, augmenting surface runoff by 2.14% and 12.72%. This was accompanied by corresponding reductions in subsurface flow of 7.43% and 10.40%, and in evapotranspiration of 10.03% and 21.65%. Interestingly, both climate and LULC changes promoted subsurface flow and evapotranspiration during the 2001–2010 period before exhibiting a declining trend in 2011–2020. The results underscore that the expansion of settlements and the reduction of forest and shrub land have intensified streamflow while lowering subsurface flow and evapotranspiration. These findings emphasize the critical need for integrated climate and land use considerations in future water resource management strategies.

**Keywords:** Watershed hydrology, Land use change impact, Scenario-based modeling, Catchment response

**Article Type:** Research Article

**Academic Editor:** Zainab Hazbavi

\*Corresponding Author, E-mail: tklohani@gmail.com

**Citation:** Werede, K.Z., Lohani, T.K., Neka, B.G., & Geremew, G.B. (2025). Modeling streamflow dynamics under climate and land use shifts using MIKE SHE in the upper Omo Gibe catchment, Ethiopia, 5 (Special Issue: Climate Change and Effects on Water and Soil), 121-148.

doi: 10.22098/mmws.2025.17906.1632

Received: ٢٤ July 2025, Received in revised form 10 August 2025, Accepted: ١٠ August 2025, Published online: 30 August 2025

*Water and Soil Management and Modeling*, Year 2025, Vol. 5, Special Issue, pp. 121-148

Publisher: University of Mohaghegh Ardabili

© Author(s)



## 1. Introduction

The complex interplay between climatic variables and land surface characteristics fundamentally drives hydrological processes. Alterations in climate and land use patterns can reshape a basin's water cycle, affecting streamflow, groundwater recharge, and soil moisture (Lucas-Borja et al., 2020). These shifts present significant challenges to water resource management, especially in data-scarce regions like Ethiopia, where a nuanced understanding of these dynamics is crucial for sustainable development (Guduru et al., 2023; Getachew et al., 2021). The Upper Omo Gibe catchment in Ethiopia is a prime example of a region facing significant hydrological challenges from concurrent climate and land use shifts, which have led to a decline in groundwater recharge and increased surface runoff (Gebremichael et al., 2024; Truneh et al., 2023). Recent research has increasingly focused on the combined effects of climate and land use changes on hydrological systems. A substantial body of work has utilized models like SWAT and HEC-HMS for large-scale assessments (Tassew et al., 2019). For example, studies in Ethiopia by Guduru et al. (2023) and Getachew et al. (2021) have used these models to assess hydrological changes. However, a growing consensus suggests that these models, despite their utility, often fail to accurately represent the fine-scale interactions between surface and subsurface water. This limitation has spurred a heightened interest in more sophisticated, fully-distributed hydrological models.

Recent research has increasingly focused on the combined effects of climate and land use changes on hydrological systems. While a substantial body of work has utilized models like SWAT and HEC-HMS for large-scale assessments, a growing consensus suggests that these models, despite their utility, often fail to accurately represent the fine-scale interactions between surface and subsurface water. This limitation has spurred a heightened interest in more sophisticated, fully-distributed hydrological models.

Numerical simulations have become an indispensable tool in this field. The MIKE SHE model, a physically-based, spatially-distributed hydrological model, has been particularly

effective. This model's process-based approach integrates surface water, groundwater, and evapotranspiration, providing a more detailed and accurate representation of hydrological complexities (Han et al., 2023). This makes it well-suited for analyzing the synergistic effects of climate and land use changes. Furthermore, several recent studies have emphasized the necessity of a holistic approach, underscoring that integrating the analysis of both climate and land use changes is essential for advancing water resource management and mitigating risks like floods and droughts (Lucas-Borja et al., 2020; Haddeland et al., 2014).

In Ethiopia, researchers have successfully applied the MIKE SHE model to address similar hydrological challenges. For instance, in the Shaya catchment, a study found that although rainfall showed no significant trend, streamflow increased significantly over two decades due to the expansion of agricultural and settlement areas (Aredo et al., 2021). Similarly, research in the Lake Tana sub-basin employed a coupled MIKE SHE/MIKE HYDRO model to forecast streamflow dynamics under climate change, confirming the model's ability to simulate future hydrological conditions (Abate et al., 2025). Most notably, a recent study by Werede et al. (2024) specifically focused on the Upper Omo Gibe catchment and found that land use changes had a significant impact on streamflow, leading to increased flows during the wet season and decreased flows during the dry season. These findings underscore the model's capability to capture the complex, localized impacts of land use change, reinforcing the need for its application in other critical catchments.

Despite these advances, a comprehensive analysis that simultaneously considers the combined effects of both climate and land use changes in the Upper Omo Gibe catchment using a high-resolution, process-based model remains a critical gap. Werede et al. (2024) focused primarily on land use change, highlighting the need for further research that integrates climate factors for a more complete understanding. This study aims to bridge this critical gap by employing the MIKE SHE model to assess the combined effects of climate change and land use alterations on streamflow in the Upper Omo Gibe

catchment. By integrating high-resolution climate and land use data, this research seeks to provide a more nuanced understanding of how these factors interact, offering valuable insights for developing more effective and adaptive water management strategies for the region.

## 2. Materials and Methods

### 2.1. Study Area and Data

The Upper Omo Gibe catchment, situated in the southwestern highlands of Ethiopia, is geographically located at 35° 36' E to 38° 34' E longitude and from 6° 25' N to 9° 24' N latitude (Figure 1). The region's topography is rugged and highly varied, with elevations ranging from 746 m to 3522 m above sea level (Figure 1). The highest elevations are found in the northern part of the catchment, contributing to diverse microclimates and ecological zones that significantly influence local hydrological processes.

The climate is characterized by a rainy season with annual rainfall estimated at 1200–1425 mm and a distinct dry season with minimal precipitation (Degefu & Bewket, 2014). Temperatures in the catchment are generally warmer in the south, with maximums ranging from 25°C to 30°C and minimums from 9°C to 12°C. The annual average temperature is 19.4°C. Covering an area of 33210 km<sup>2</sup>, the catchment is drained by major rivers, including the Gibe, Omo Gibe, and Gilgel Gibe, as well as numerous tributaries. This extensive river network supports downstream ecosystems and human settlements, providing water for agriculture, drinking, and hydroelectric power generation. The Omo basin's substantial potential for irrigation and hydropower development, along with its rich biodiversity, highlights its ecological and economic importance (Awulachew et al., 2007).

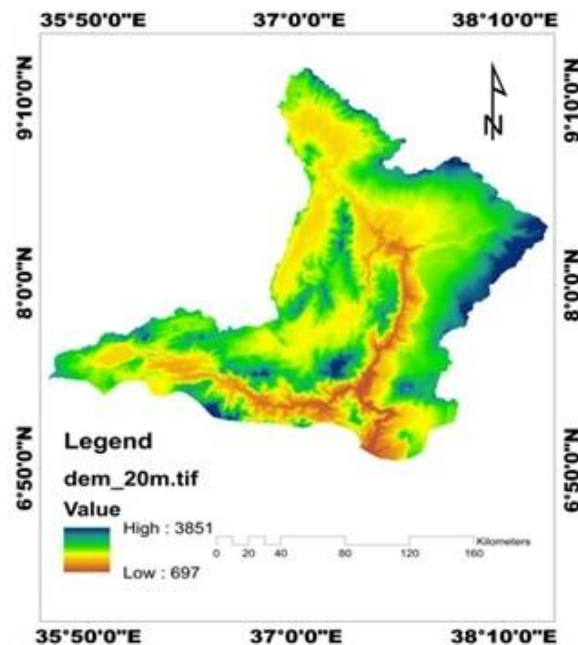


**Figure 1.** The digital elevation model of the upper Omo Gibe catchment.

#### 2.1.1. Hydro-meteorological data acquisition and interpretation

Daily climatological data, including precipitation and temperature extremes (minimum and maximum), were obtained from the Ethiopian National Meteorological Agency (EMA) from 1990 to 2020 (Table 1). This data was collected

from nine meteorological stations, a common practice in regions with sparse monitoring networks to address data continuity and station establishment challenges (Awulachew et al., 2007). The selection criteria for these datasets were based on data completeness, long-term availability, and suitability for hydrological

model analysis, which are critical steps for reducing uncertainty in model outputs (Han et al., 2023). Additionally, streamflow data for the period of 1990 to 2014 were acquired from the Hydrology Department of the Ethiopian Ministry of Water and Energy (MoWE). Following standard hydrological modeling procedures, reference evapotranspiration was computed using the widely accepted Penman-Monteith method, a method known for its accuracy and robustness in various climatic conditions (Allen et al., 1998). The entire dataset was subjected to a thorough screening process to identify and address outliers and incomplete data, ensuring the quality and reliability of the inputs for the MIKE SHE model

(Ayana et al., 2021). This rigorous data preparation is essential for generating reliable simulations of catchment processes (Butts et al., 2004). Corrections were made by cross-referencing records with data from nearby stations to ensure accuracy. Catchments and monitoring stations were chosen based on the completeness and quality of available data, with only time series containing less than 10% missing values for daily streamflow and monthly weather records included in the analysis. This rigorous selection and validation process helped maintain data integrity, ensuring that the dataset used for analysis was both comprehensive and reliable (Milly et al., 2005; WMO, 2008).

**Table 1. Hydro-meteorological stations in the upper Omo Gibe Basin.**

S.No	Station name	Latitude (deg.)	Longitude (deg.)	Altitude (masl)	Precipitation (mm)	Temperature maximum (°C)	Temperature minimum (°C)	Period	
1	Assendabo	7.77	37.23	1770	√	√	√	1990	2020
2	Hossana	7.55	37.78	1729	√	√	√	1990	2020
3	Jimma	7.67	36.83	1736	√	√	√	1990	2020
4	Lemugenet	8.1	36.96	1688	√	√	√	1990	2020
5	Sekoru	7.93	37.43	1855	√	√	√	1990	2020
6	Shebe	7.52	36.52	1781	√	√	√	1990	2020
7	Woliso	8.55	37.98	2063	√	√	√	1990	2020
8	Wolita	7.01	37.75	1869	√	√	√	1990	2020
9	Wolkite	8.28	37.77	1875	√	√	√	1990	2020
10	Abelity	7.92	37.4	-	-	-	-	1990	2014

\*\* The numbers from 1 to 9 represent meteorological stations, and 10 represents hydrological stations

### 2.1.2. Spatial data sources and analysis inputs

Accurate simulations in hydrological modeling, such as those using the MIKE SHE model, rely on high-resolution spatial data for representing the intricate spatial variability in terrain, land cover, and soil properties within the watershed (Talib & Randhir, 2017). The 30-meter resolution Digital Elevation Model (DEM) and multi-temporal Landsat imagery, sourced from the USGS Earth Explorer website, provide crucial inputs for this purpose. Detailed spatial data, like those presented in Table 3 and Figure 2a, aid in capturing elevation-dependent hydrological processes, which are critical for flow direction and accumulation, as noted by studies such as Kasei et al. (2010) and Beck et al. (2018). The Omo-Gibe basin soils widely comprise Nitrosols soil, which are deep, red or reddish brown, and well-drained, and are the most productive soils of Ethiopia. However, soil degradation threatens the

(Nitrosols) productive capacity. Nitrosols soil is found mainly in eastern Africa at higher altitudes (FAO, 2001) and is the dominant soil in the Ethiopian highland, especially in the Western and southwestern part of the country (Elias, 2017). Nitrosols are widely spread in the upper part of the basin.

**Table 2. Soil type distribution by area and coverage in the Upper Omo Basin.**

Soil Type	Coverage (%)	Area (km <sup>2</sup> )
Eutric Nitrosols	77.98%	25,897.55
Eutric Cambisols	8.75%	2,906.44
Humic Cambisols	6.63%	2,204.24
Ochric Andosols	3.28%	1,090.11
Pellic Vertisols	2.56%	850.74
Plinthic Ferralsols	0.80%	260.92

The availability of multi-temporal Landsat images enhances the model's capability to integrate land cover changes over time, capturing the dynamic influences of vegetation cover and land use on runoff and infiltration rates (Xia et al., 2020). By covering different temporal and spatial scales, these data sources help to ensure the representativeness and flexibility needed for reliable MIKE SHE simulations. For instance, Tarekegn et al. (2021) emphasize that high-resolution data significantly improve model calibration and validation, allowing for better hydrological predictions, especially in regions with varied topography and land cover. Moreover, the inclusion of a soil map from the Ethiopian Ministry of Water and Energy (MoWE), or collaborating government bodies like the Ministry of Agriculture, adds a crucial layer of spatial accuracy (Table 2). This data is

essential for determining soil-specific hydraulic characteristics, such as porosity and permeability, which govern soil water retention and movement within the model. Recent studies in the Ethiopian highlands have confirmed the significant influence of these soil parameters on hydrological simulations (Berhanu et al., 2013; Truneh et al., 2023). By leveraging such diverse data sources, this study ensures model accuracy and reproducibility, as comprehensive datasets allow researchers to validate the MIKE SHE model against observed hydrological patterns in Ethiopia's variable landscapes (Han et al., 2023; Butts et al., 2004). This rigorous approach is particularly important for capturing the complex surface and subsurface water interactions that are key to understanding the catchment's response to environmental changes.

**Table 3. Material sources used in land use and land cover classification.**

S.no.	Image	Sources	Resolution (m)	Sensor type	Path/row	Acquisition Date
1	Landsat5	<a href="http://earthexplore.usgs.gov/">http://earthexplore.usgs.gov/</a>	30	TM	169/055	January 1990
2	Landsat7	<a href="http://earthexplore.usgs.gov/">http://earthexplore.usgs.gov/</a>	30	ETM	169/055	January 2005
3	Landsat8	<a href="http://earthexplore.usgs.gov/">http://earthexplore.usgs.gov/</a>	30	OLI	169/055	February 2020

The elevation ranges from 697 m to 3851 m. The highest elevation occurs in patches ranging beyond 2580 m, 1800 m – 2100 m, all along the northern, eastern, and southern frontiers, some parts of the western and central regions. The

northern, central and some small patches have an average elevation of 1500 m (Figure 2b).

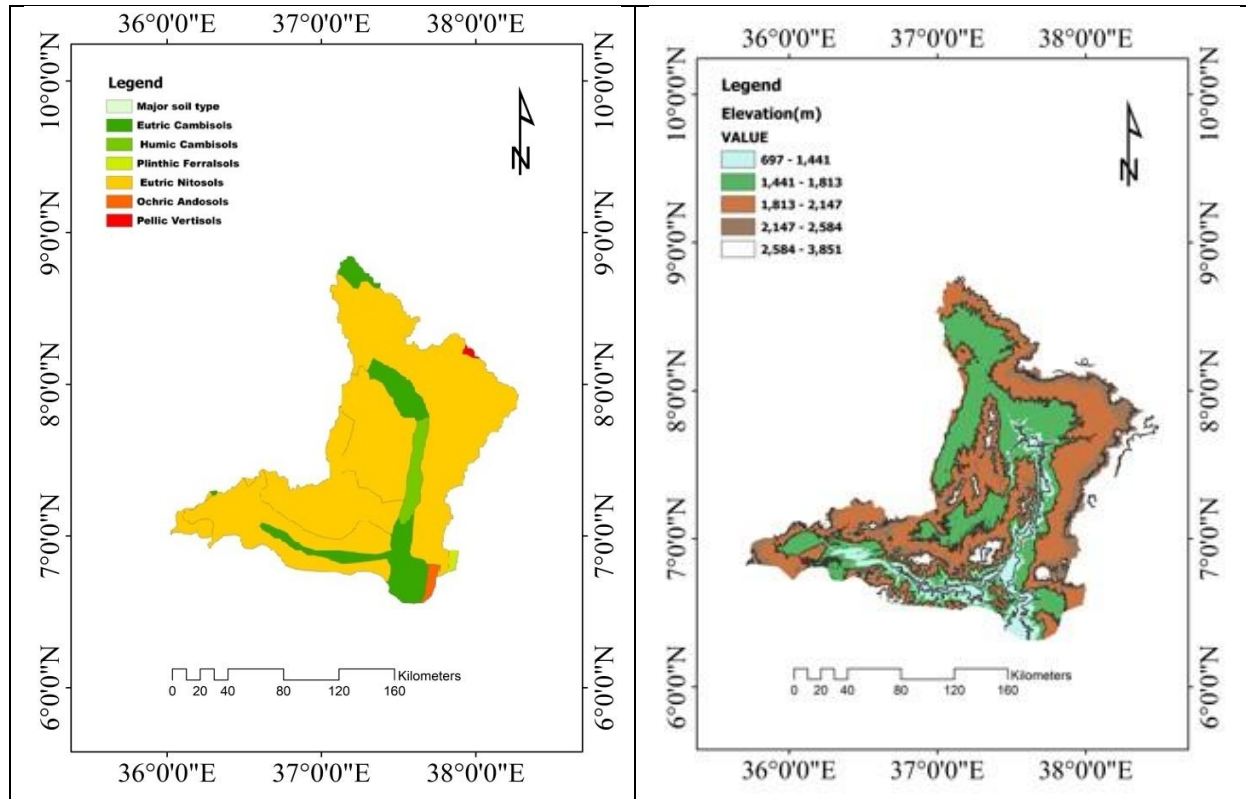


Figure 2. left) Soil map of the study area; right) topographic map of the study area

## 2.2. Methodology

### 2.2.1. LULC type accuracy assessment

This method evaluates the accuracy of land use and land cover (LULC) classifications derived from remote sensing and GIS techniques. This involved a comparison of our classified LULC map against a robust set of reference data, a standard procedure for ensuring the reliability of land cover products (Congalton & Green, 2019). The reference data was meticulously compiled from a combination of field surveys and high-resolution imagery from platforms like Google Earth.

To ensure a comprehensive assessment, we collected fifty ground-truth points for each land cover category. These points were then cross-referenced with the corresponding pixel's assigned classification to gauge its accuracy against our reference sources. We utilized two widely accepted metrics for this evaluation: overall accuracy and the Kappa coefficient (Foody, 2002). Overall accuracy provided a straightforward percentage of correctly classified pixels across the entire study area. In contrast, the Kappa coefficient, a more sophisticated statistical

measure, quantified the agreement between our classified image and the ground truth data while accounting for the possibility of random chance agreement. This dual approach ensured a rigorous assessment of our LULC classification. A kappa coefficient of 1 denotes perfect agreement, while 0 suggests agreement equivalent to chance, and negative values indicate agreement worse than chance (Anderson, 1976; Ismail & Jusoff, 2008) (Equation 1 and Equation 2)

Overall Accuracy

$$= \frac{\text{Number of correctly classified pixels}}{\text{Total number of pixels}} \times 100 \quad (1)$$

Kappa (K)

$$= \frac{m \sum_{i=1}^n x_{ii} - \sum_{i=1}^n (x_{i+} \times x_{+i})}{m^2 - \sum_{i=1}^n (x_{i+} \times x_{+i})} \times 100 \quad (2)$$

where,  $n$  represents the total number of land cover types,  $m$  denotes the overall number of sample pixels, the term  $x_{ii}$  indicates the number of pixels correctly classified as land cover type  $i$ ,  $x_{i+}$  denotes the count of type  $i$  pixels within the validation sample sets, and  $x_{+i}$  represents the number of type  $i$  pixels in the reference corresponding to the sample set.

### 2.2.2. Hydrological MIKE SHE model descriptions

The MIKE SHE model, developed by the Danish Hydraulic Institute (DHI), is recognized as a highly comprehensive tool in hydrological modeling for its extensive capabilities in simulating critical land-based hydrological processes (DHI, 2023; Graham & Butts, 2005). This model is fully distributed and physically based, enabling it to accurately capture interactions within the hydrological cycle, such as those between surface water and groundwater systems, across various watershed and basin scales. The model's strength lies in its ability to integrate a wide range of hydrological processes, including precipitation, evapotranspiration, surface runoff, infiltration, and streamflow routing, as well as groundwater flow, making it highly effective for applications in water resource management, flood forecasting, and ecosystem research (Butts et al., 2004; Singh & Woolhiser, 2002).

MIKE SHE's deterministic framework utilizes orthogonal grid networks to spatially distribute watershed parameters, climate data, and hydrological responses, allowing fine-scale spatial allocation within each grid cell, and extending to sub-surface layers to model vertical and lateral flows (Graham & Butts, 2005). The model integrates hydrological principles, applying the Saint-Venant equations for channel and overland flow, Richards' equation for unsaturated zone flow, and the finite difference method for saturated groundwater flows. Evapotranspiration is modeled using methods such as the Kristensen and Jensen approach, highlighting MIKE SHE's application of physically robust methods to support high-fidelity simulations of real-world hydrological dynamics (Abbott et al., 1986).

Specialized modules within MIKE SHE extend its versatility, including the Water Quality (AD), Sediment Transport (SE), Dual Porosity (DP), Geochemical Processes (GC), Crop Growth and Nitrogen (CN), and Irrigation (IR) modules, which provide detailed modeling of additional processes such as pollutant transport, geochemical interactions, and agricultural impacts within the hydrological system (Singh & Woolhiser, 2002). These modules make MIKE

SHE particularly suitable for integrated catchment management where both quantity and quality aspects of water resources need to be considered holistically.

### 2.2.3. MIKE SHE model input data

The MIKE SHE model relies heavily on a diverse array of critical input datasets to effectively simulate hydrological processes with precision. These foundational inputs encompass meteorological variables such as precipitation, temperature, streamflow, and evapotranspiration to comprehend the dynamics of water movement throughout the watershed. Beyond meteorological data, detailed information on soil properties assumes a pivotal role. Parameters like infiltration rates and hydraulic conductivity profoundly influence water permeation through the soil profile, shaping runoff patterns and groundwater recharge dynamics. Accurate representations of land use and land cover are equally indispensable inputs. They dictate surface runoff characteristics, evapotranspiration rates, and the overall water balance within the watershed. The topography of the study area, encompassing elevation and slope, exerts a significant influence on hydrological responses, affecting flow velocities and accumulation areas. Ensuring the reliability and accuracy of these input datasets is paramount to the MIKE SHE model's efficacy. Calibration involves meticulous adjustment of model parameters to closely align simulated outputs with observed data. Concurrently, validation confirms the model's ability to replicate observed hydrological behaviors under varying environmental conditions. This rigorous calibration and validation process enhances the model's credibility, enabling it to furnish dependable predictions regarding water flow dynamics, availability, and quality. By providing robust simulations backed by calibrated and validated inputs, the MIKE SHE model supports informed decision-making processes that are crucial for effective water resource management. It serves as a valuable tool for stakeholders ranging from researchers and engineers to policymakers, facilitating sustainable water resource management strategies tailored to local hydrological conditions.



### 2.2.4. Model calibration and validation

The development and evaluation of hydrological models involve critical phases of calibration and validation, essential for ensuring the accuracy and reliability of model predictions. Calibration focuses on refining model parameters to closely align simulated outputs with observed data, while validation verifies the model's performance under conditions not used during calibration. In this study, the MIKE SHE model underwent meticulous calibration and validation processes using streamflow data from the Abeltiy gauge station. Calibration spans from 1990 to 2004 and included sensitivity analysis to assess how adjustments to parameters like micro-pores bypass flow ( $B_c$ ), Manning's roughness coefficient ( $n$ ), drainage depth ( $D_D$ ), Saturated hydraulic conductivities ( $K_s$ ) and Drainage time ( $D_t$ ), influenced model simulations. Adjustments were made within reasonable ranges sourced from manuals, a global digital soil map, and the SWAT database, given the limited local data availability.

Following the parameter adjustments, the model's performance was validated using independent data from 2005 to 2014. Both manual and automatic calibration methods were employed to compare monthly streamflow outputs from the model with observed data, ensuring an accuracy assessment. The sensitivity analysis conducted with the MIKE SHE model not only enhances understanding of hydrological processes but also enhances model precision by pinpointing influential parameters. This analysis aids stakeholders, including researchers, engineers, and policymakers, in making informed decisions about water resource management, flood mitigation, and ecosystem conservation tailored to specific local hydrological conditions.

### 2.2.5. Model statistical evaluation

Evaluating the performance of hydrological models involves comparing simulated outputs with observed data to assess how accurately a model reproduces hydrological processes (Moriassi et al., 2007). For this study, we statistically compared observed flow measurements from gauging stations with simulated flows from the MIKE SHE model. This approach is a standard and essential step for

validating hydrological models (Butts et al., 2004). We employed several standard metrics to evaluate the model's performance, each providing a different insight into its accuracy and reliability. These metrics included the Nash-Sutcliffe Efficiency (NSE), which assesses the model's predictive skill relative to the mean of the observed data (Nash & Sutcliffe, 1970); the correlation coefficient (R), which measures the linear relationship between observed and simulated flows; and the Root Mean Square Error (RMSE), which quantifies the average magnitude of the errors (Moriassi et al., 2007). Together, these metrics allowed for a comprehensive and robust evaluation of the model's ability to reproduce the catchment's hydrological behavior. The Nash-Sutcliffe Efficiency (NSE) is a widely used statistic that measures how well simulated data represent observed data variability. Values for NSE range from negative infinity to 1, with values close to 1 indicating a better match between simulated and observed data, a critical standard for model validation in hydrology. The correlation coefficient (R) is another important metric, quantifying the strength and direction of the linear relationship between observed and simulated data. R values range from -1 to 1, with values near 1 signifying a strong positive correlation and values near -1 indicating a strong negative correlation, while  $R = 0$  suggests no linear correlation between data sets (Legates & McCabe, 1999).

Lastly, the Root Mean Square Error (RMSE) serves as a measure of precision, calculating the average magnitude of differences between observed and simulated values. Lower RMSE values reflect higher model accuracy, with values close to zero indicating minimal errors and a good fit. Together, these metrics enable a robust evaluation of the MIKE SHE model's ability to replicate hydrological processes, offering essential insights for water resource management and environmental studies (Gupta et al., 2009). The formulas for calculating statistical tests for hydrological model performance (Equation 3 – Equation 5).

$$NSE = 1 - \frac{\sum_{i=1}^n (Q_i - S_i)^2}{\sum_{i=1}^n (Q_i - \hat{O}_i)^2} \quad (3)$$



$$R = \frac{\sqrt{\sum_{i=1}^n (S_{i,t} - \hat{O}_{i,t})^2}}{\sqrt{\sum_{i=1}^n (Q_{i,t} - \hat{O}_{i,t})^2}} \quad (4)$$

$$RMSE = \frac{\sqrt{\sum_{i=1}^n (Q_{i,t} - S_{i,t})^2}}{n} \quad (5)$$

where, at time step  $i$ ,  $Q_i$  represents the observed value,  $S_i$  denotes the simulated value,  $\hat{O}_i$  stands for the mean of the observed values,  $S_{i,t}$  indicates simulated flow,  $Q_{i,t}$  represents observed flow,  $\hat{O}_{i,t}$  is the mean of observations at location  $i$ , “ $t$ ” denotes the  $i^{\text{th}}$  location at time  $t$ , and “ $n$ ” refers to the total number of observations.

### 2.2.6. Simulation scenario development for impact assessment

Scenario-based simulations were undertaken to evaluate the individual and combined impacts of climate and land use changes on streamflow, utilizing diverse meteorological datasets and land use/land cover (LULC) maps. The study assessed how climate change-induced variations in precipitation patterns, temperature regimes, and evapotranspiration rates, derived from different periods of meteorological data, interacted with alterations in land cover types and land use patterns. These changes included the expansion of built-up areas, deforestation, agricultural

intensification, and modifications in water bodies (Ortiz et al., 2021).

To analyze the effects of climate and LULC changes on hydrological processes, a fixed-changing approach was adopted (Yin et al., 2017). Meteorological data spanning 1990 to 2020 were divided into three distinct periods: 1990-2000, 2001-2010, and 2011-2020. These periods were then combined with LULC maps from three key years: 1990, 2005, and 2020, respectively, to develop three core simulation scenarios (Table 4).

This segmentation allowed for the development of three representative scenarios to explore the combined effects of climate and LULC changes on runoff patterns over the study period. By comparing these scenarios to the baseline period, the study effectively captured the influence of integrated climate and land use changes on hydrological systems. The results contribute valuable insights into how these factors impact water resource management strategies, guiding future planning and adaptation efforts in the context of ongoing climate and land use transformations (Shang et al., 2019; Kumar et al., 2022; Malede et al., 2023). Table 3 presents a series of simulated scenarios for the period from 1990 to 2020, aiming to assess the impacts of climate and land use changes on hydrological systems.

**Table 4. Detailed climate and land use/land cover change Scenarios.**

Scenario	Meteorological data	Land use land cover map	Scenario description
SC1	1990-2000	1990	Reference period with baseline climate (1990-2000) and land use (1990) conditions
SC 2	2001-2010	1990	Assumed scenario with climate change (2001-2010) and land use changes (2005)
SC 3	2011-2020	1990	Assumed scenario with climate change (2011-2020) and land use changes (2020)

### Explanation of the Three Core Scenarios:

**1- SC1:** This scenario serves as the baseline, with meteorological data from 1990-2000 and the LULC from 1990, representing the historical reference period.

**2- SC2:** This scenario assumes climate change based on the 2001-2010 period, with the land

use/land cover map from 2005. It reflects hypothetical land and climate changes during this period.

**3- SC3:** This scenario reflects a more recent period (2011-2020) with assumed LULC from 2020, showing how the most recent climate data interacts with the latest land use changes.

This simplified approach keeps the focus on three distinct periods: the baseline (SC1), a period with moderate climate and land use change (SC2), and a period with more recent and significant changes (SC3). The study employs a specific formula to calculate the relative contributions of climate, land use/change, and their combined effects on hydrological flows, enabling an evaluation of differences in simulated mean discharges across scenarios. Equations (6) – Equation (8) quantified the percentage changes in hydrological flows due to the separate and combined effects of climate, land use, and land cover (LULC) changes (Kumar et al., 2022).

$$\Delta q_{iso, Climate} = \left( \frac{SC2 - SC1}{SC1} \right) \times 100 \quad (6)$$

$$\Delta q_{iso, LULC} = \left( \frac{SC4 - SC1}{SC1} \right) \times 100 \quad (7)$$

$$\Delta q_{Comb} = \left( \frac{SC5 - SC1}{SC1} \right) \times 100 \quad (8)$$

where,  $\Delta q$  represents the change in annual runoff simulated during the effects of climate, LULC, and combined on hydrological processes.  $\Delta q_{Comb}$  = combined impact

### 3. Results and Discussion

#### 3.1. Detection of land use and land cover changes

The analysis of land use and land cover (LULC) changes in the Upper Omo Gibe Basin from 1990 to 2020 reveals significant transformations driven by agricultural expansion, urbanization, and hydropower development. The historical LULC maps (Figure 3a–3c) illustrate these changes,

while Table 4 quantifies the extent and percentage shifts in different land cover categories over three decades.

A key observation from the study is the substantial decline in forest and shrub land areas. Forest cover decreased from 17.9% in 1990 to 8.92% in 2020, while shrub land declined from 13.81% to 2.78% during the same period. These losses were primarily driven by agricultural expansion and settlement growth, as agricultural land increased from 66.09% in 1990 to 84.43% in 2020. Population growth and economic activities have led to the conversion of natural vegetation into cropland and built-up areas, significantly altering the hydrological balance of the basin (Derebe et al., 2022; Lukas et al., 2023). Studies by Belay & Mengistu (2021) and Gitima et al. (2023) confirm that agricultural expansion is the primary driver of land cover change in Ethiopia's river basins, causing notable reductions in forest cover and biodiversity.

Another notable change is the expansion of water bodies, which grew from 0.39% (131.22 km<sup>2</sup>) in 1990 to 1.06% (353.89 km<sup>2</sup>) in 2020, an increase of approximately 169.69%. This expansion is primarily attributed to the construction of the Gibe-I, Gibe-II, and Gibe-III hydropower dams. These reservoirs have substantially increased the surface water storage capacity in the basin, influencing streamflow dynamics and regional water availability (Taye et al., 2018; Hussen et al., 2021). The impoundment of water in these hydropower projects has not only contributed to the observed increase in water bodies but has also altered downstream hydrological processes by regulating flow regimes and modifying seasonal discharge patterns (Woldesenbet et al., 2020).

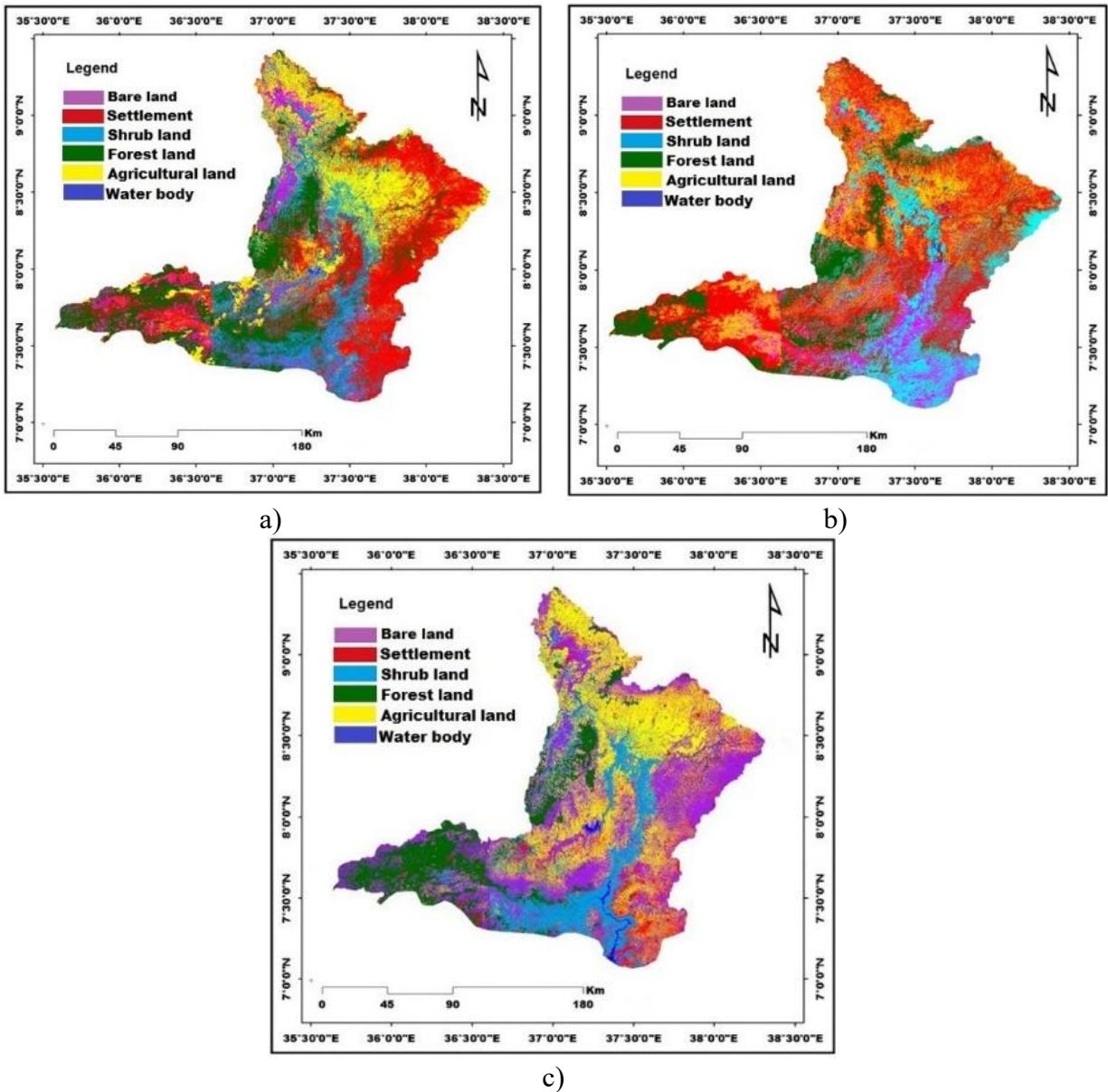


**Figure 3. a, b, and c refer to land use and land cover distributions for the years 1990, 2005, and 2020, respectively.**

Table 5 provides a detailed breakdown of the percentage changes in different LULC classes. Agricultural land remains the dominant land use, while forest and shrub land continue to decline. The steady rise in settlement areas (from 1.01% in 1990 to 1.83% in 2020) highlights the impact of human activities on landscape transformation (Malede et al., 2023). These LULC changes have profound implications for hydrological processes, particularly in terms of runoff generation, evapotranspiration, and groundwater recharge. The expansion of cropland and urban

areas has likely contributed to increased surface runoff and reduced infiltration rates, exacerbating flood risks in certain regions (Shang et al., 2019; Kumar et al., 2022). Meanwhile, the rise in water bodies due to hydropower developments underscores the role of large-scale infrastructure projects in reshaping the basin's hydrological characteristics (Teshome & Zhang, 2019). Overall, these findings emphasize the need for sustainable land and water resource management strategies to mitigate adverse environmental impacts while supporting economic growth and

energy production in the region. Integrated land and water management approaches such as afforestation, soil conservation, and regulated

urban planning are crucial to balancing development needs with ecological sustainability (Gebrehiwot et al., 2022; Lukas et al., 2023).

**Table 5. Extent and percentage alterations in LULC (1990-2020)**

LULC Classes	1990		2005		2020		Net Change (1990-2020)	
	Area(km <sup>2</sup> )	Area (%)	Area (km <sup>2</sup> )	Area (%)	Area (km <sup>2</sup> )	Area (%)	Area (km <sup>2</sup> )	Percent (%)
Bare land	260.46	0.78	193.06	0.58	323.64	0.98	63.18	24.25708
Settlement	335.43	1.01	585.38	1.76	607.14	1.83	271.71	81.00349
Shrub land	4,585.57	13.81	1,329.13	4.0	923.93	2.78	-3661.64	-79.8514
Forest	5946.01	17.9	3934.37	11.85	2962.63	8.92	-2983.38	-50.1745
Agriculture	21951.6	66.09	26977.48	81.23	28039.06	84.43	6087.46	27.73128
Water body	131.22	0.39	190.87	0.58	353.89	1.06	222.67	169.6921
Total	33,210.29	100	33,210.29	100	33,210.29	100		

### 3.2 Assessment of the accuracy of classified LULC

The classified LULC data were found to be highly accurate, validating the reliability of the data utilized in this study. Ensuring high accuracy is crucial as it underpins the analyses and conclusions regarding the impacts of land use and climate change on runoff flow in the upper Omo Gibe reservoir catchment. The overall accuracy rates for the LULC were 90.76% for 1990, 91.06% for 2005, and 92.24% for 2020, surpassing the minimum threshold of 85% (Lu & Weng, 2007; Nath *et al.*, 2014; Congalton &

Green, 2019). Additionally, the Kappa coefficients indicated the strength of agreement between the classified LULC data and the reference data were noted as 0.89 for 1990, 0.88 for 2005, and 0.89 for 2020. These high values reflect a robust and almost perfect agreement, confirming the classification method's reliability. This level of accuracy is vital for assessing the hydrological impacts of land use and climate change, providing a solid empirical foundation for the study's findings related to runoff flow changes (Table 6).

**Table 6. Accuracy assessment of LULC map classification of 1990, 2005, and 2020**

Land use classes	LULC map of 1990		LULC map of 2005		LULC map of 2020	
	Producer accuracy (%)	User's accuracy (%)	Producer accuracy (%)	User's accuracy (%)	Producer accuracy (%)	User's accuracy (%)
Bare land	95	88	88	92	85	88
Settlement	100	75	100	100	100	100
Shrub land	94	86	87	94	94	97
Forest	100	85	90	100	86	100
Agricultural land	90	100	92	85	90	93
Water body	91	95	100	90	100	100
Overall accuracy (%)		90.76		91.06		92.24
Kappa statistic (%)		0.89		0.88		0.89

### 3.3 Assessment of the MIKE SHE Model

To ensure accurate simulation of runoff flow dynamics in the study area, the MIKE SHE model underwent thorough calibration and validation

using observed hydrological data, including streamflow measurements. Calibration involved fine-tuning model parameters to minimize differences between observed and simulated hydrological variables. Validation assessed the

model's reliability using independent datasets. The split-sample calibration-validation method was employed, dividing the data into distinct periods for calibration and validation. The model was calibrated with monthly streamflow data from 1990 to 2004 for the upper Omo catchment. Data from 2005 to 2020 were then used for validation to evaluate the model's accuracy.

To prevent over-parameterization, which can complicate the model, only a limited number of parameters were adjusted during calibration. This approach is particularly crucial for a distributed model like MIKE SHE, where balancing model complexity with parameter manageability is key to ensuring robust and reliable simulations. The calibration process involved fine-tuning several parameters, including the surface roughness coefficient or Manning's ( $M$ ), micro pores bypass flow ( $B_c$ ), drainage depth ( $D_D$ ), Saturated hydraulic conductivities ( $K_s$ ), and Drainage time ( $D_t$ ). The default and adjusted values are presented in Table 6.

Analysis showed that Manning's  $M$  and hydraulic conductivity were the most critical parameters influencing the hydrograph. According to Paudel & Benjankar (2022), these parameters significantly impact surface runoff, necessitating precise calibration and validation for accurate hydrological modeling and effective water resource management. For instance, as Manning's  $M$  increases, overland flow speed rises, while subsurface drainage flow decreases. Micropore bypass flow significantly influences runoff dynamics by allowing water to quickly move through small channels in the soil, bypassing the slower process of matrix flow. This rapid movement can lead to increased surface runoff and altered hydrograph responses. Drainage time and depth also moderately affect simulated discharge by determining how quickly water can percolate through the soil and contribute to subsurface flow. Studies, including those by Vázquez et al. (2002), Sahoo et al. (2006a, 2006b), Zhang et al. (2008), Loliyana & Patel (2018), and Aredo et al. (2021), have consistently identified the surface roughness coefficient and hydraulic conductivity as critical parameters impacting surface runoff. These studies highlight that precise calibration of these parameters is essential for accurate hydrological modeling and

effective water resource management. Surface roughness, represented by Manning's coefficient, influences the velocity of overland flow, while hydraulic conductivity controls the infiltration rate and subsequent subsurface flow, both crucial for simulating the hydrological response accurately.

Saturated zone hydraulic conductivities play a vital role in influencing both streamflow and base flow by governing water movement in both vertical and horizontal directions within the subsurface. Vertical hydraulic conductivity is critical in determining the rate at which water infiltrates deeper into the aquifers, facilitating groundwater recharge. This downward movement is essential for sustaining base flow, particularly during dry periods when groundwater contributes to streamflow. Conversely, horizontal hydraulic conductivity primarily influences base flow, as it controls the lateral movement of water through soil and rock layers. Unlike vertical conductivity, horizontal conductivity has minimal effect on surface runoff due to the sloping topography of the study area, which reduces its impact on surface water flow dynamics.

To improve the fidelity of model outputs relative to observed data, hydrogeological parameters were carefully calibrated and optimized. This precise calibration allowed the model to produce a realistic representation of total discharge. Parameters such as macropore bypass flow, drainage time, and drainage depth were adjusted primarily to reduce computational simulation time without compromising the accuracy of surface water simulation. These factors are especially relevant during wet soil conditions, where they facilitate the movement of water into subsurface layers, thereby promoting subsurface flow while minimally affecting surface runoff dynamics (Guzha et al., 2018). This comprehensive approach helps ensure the hydrological model accurately reflects the natural hydrological processes, accounting for both subsurface and surface water interactions.

For the calibration process, the observed monthly streamflow data at the Abeli gauging station were compared with the streamflow simulated by the MIKE SHE model, as shown in Figures 4 and 5. The model was run for the period from 1990 to

2000, utilizing land use data from 1990. Figure 4 illustrates that the peak values of the simulated monthly streamflow align closely with the observed values, despite some differences in magnitudes. The satisfactory R-value of 0.82 and the NSE model efficiency of 0.83, as presented in Table 7, indicate a strong correspondence between the observed and simulated streamflow. This demonstrates that the MIKE SHE model produced reliable results for the watershed's monthly discharge, validating its application for further analysis. The model showed satisfactory

performance during both the calibration and validation phases, with a good match between observed and simulated streamflow values. Figure 5 further reveals that for lower observed streamflow values, the simulated streamflow values are uniformly distributed along a one-to-one line, signifying a high level of accuracy. However, for higher discharge values, the model slightly underestimated the simulated values, indicating minor discrepancies in replicating peak flow events.

**Table 7. Calibrated values for sensitive parameters in the MIKE SHE model used for simulation.**

S.no	Parameters description	Unit	Range value	Fitted value
1	Manning's number (M)	$M^{1/3}/s$	4.0-25.0	10.0
2	Micro pores by-pass flow ( $B_c$ )	-	0.3-0.8	0.7
3	Drainage depth ( $D_D$ )	m	1.0-1.5	1.1
4	Saturated hydraulic conductivities ( $K_s$ )	m/s	$1 \times 10^{-6} - 1 \times 10^{-3}$	$8.73 \times 10^{-6}$
5	Drainage time ( $D_t$ )	$s^{-1}$	$3 \times 10^{-6} - 5 \times 10^{-6}$	$4 \times 10^{-6}$

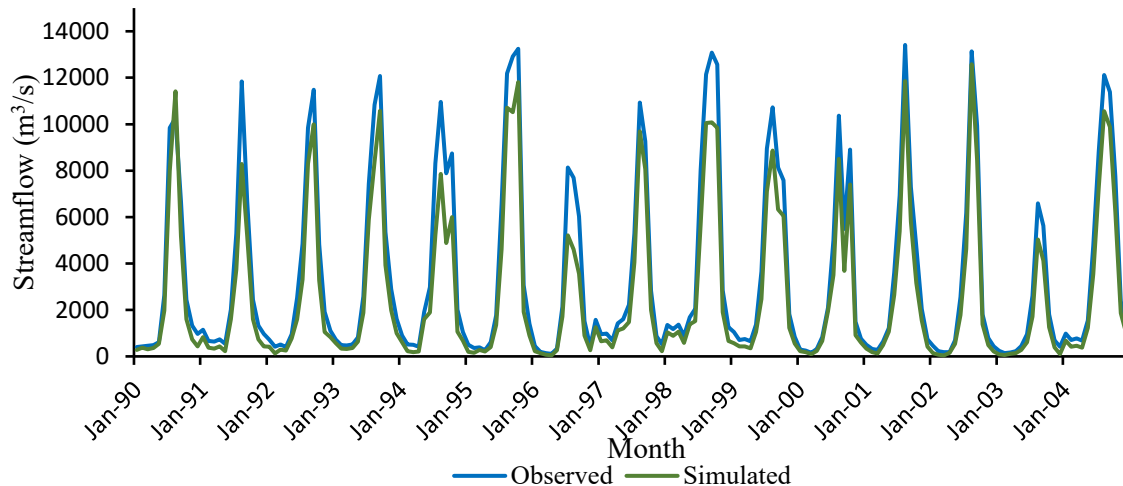


**Figure 4. Observed and simulated streamflow data were compared for model calibration (1990-2004)**

The peak of the simulated streamflow being consistently lower than the observed streamflow can be attributed to several potential factors, particularly related to model calibration and the representation of hydrological processes. The quality and resolution of the input meteorological data (such as precipitation and temperature) can

significantly impact the accuracy of peak flow simulations. If the rainfall data is too coarse in either space or time, the model may miss localized, intense rainfall events that contribute to higher peaks. Additionally, missing or inaccurate high-intensity rainfall data can lead to an underestimation of peak flow.

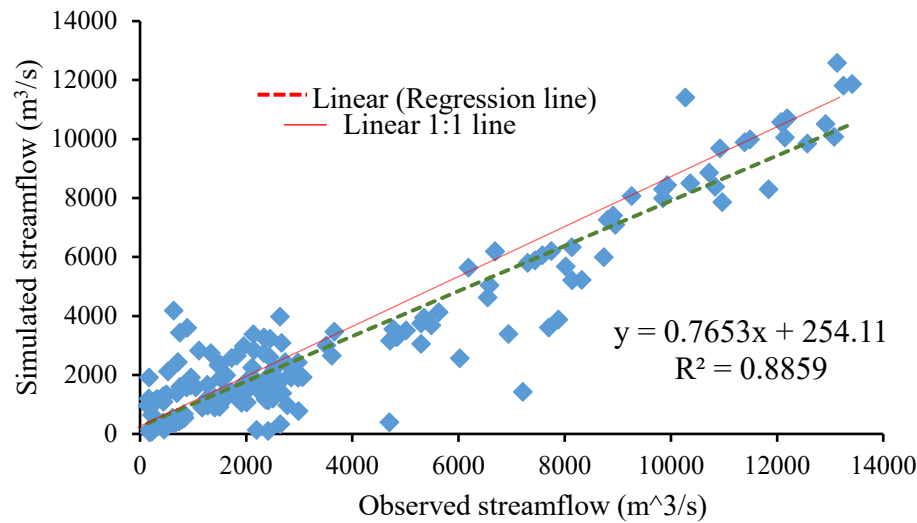


**Figure 5. Scatter plot comparing observed and simulated streamflow during the calibration period (1990–2004).**

Table 7 presents the statistical evaluation illustrating a strong relationship between observed and simulated streamflow for the years analyzed. During the model calibration period (1990–2004), the correlation coefficient (R) was 0.82, and the Nash-Sutcliffe Efficiency (NSE) was 0.83, indicating a strong match between the observed and simulated streamflow data. For the validation period (2005–2020), the correlation coefficient and NSE were 0.81 and 0.80, respectively. These values demonstrate a close agreement between the observed and simulated monthly streamflow data during both periods (Moriasi et al., 2007), affirming the model's reliability. The high correlation coefficients and NSE values suggest that the model can accurately simulate streamflow patterns, thereby justifying its use for further hydrological analysis in the watershed. These results underscore the model's robustness in capturing the dynamics of streamflow, essential for effective water resource management and planning. To further validate the model, the calibrated MIKE SHE model was tested with a new dataset. This involved using observed streamflow data from 2005 to 2014 and corresponding land use data from 2005 for the upper Omo catchment. The results of this validation are presented in Figures 6 and 7. These figures illustrate a strong agreement between observed and simulated monthly streamflow, indicating the model's reliability in predicting streamflow for this period and region. Figure 7

shows that the majority of the data points for lower discharge values are uniformly distributed around the 1:1 line, suggesting a high degree of accuracy.

**Table 8. Statistical evaluation of observed versus simulated monthly streamflow data during both the calibration and validation periods**

Period	Statistical index	Value
Calibration(1990-2004)	NSE	0.83
	R	0.82
	RMSE	2.69
Validation (2005-2014)	NSE	0.80
	R	0.81
	RMSE	3.70

However, for higher discharge values, the simulated streamflow slightly underestimates the observed values, as the points fall below the 1:1 line. This indicates that while the model accurately captures overall flow patterns, it tends to underestimate peak flows slightly. The successful calibration and validation of the MIKE SHE model demonstrate its robustness and suitability for assessing the impacts of land use and land cover (LULC) changes and climate change on water balance components. This model can thus be effectively used to predict future hydrological responses under various scenarios, providing valuable insights for water resource management and planning.



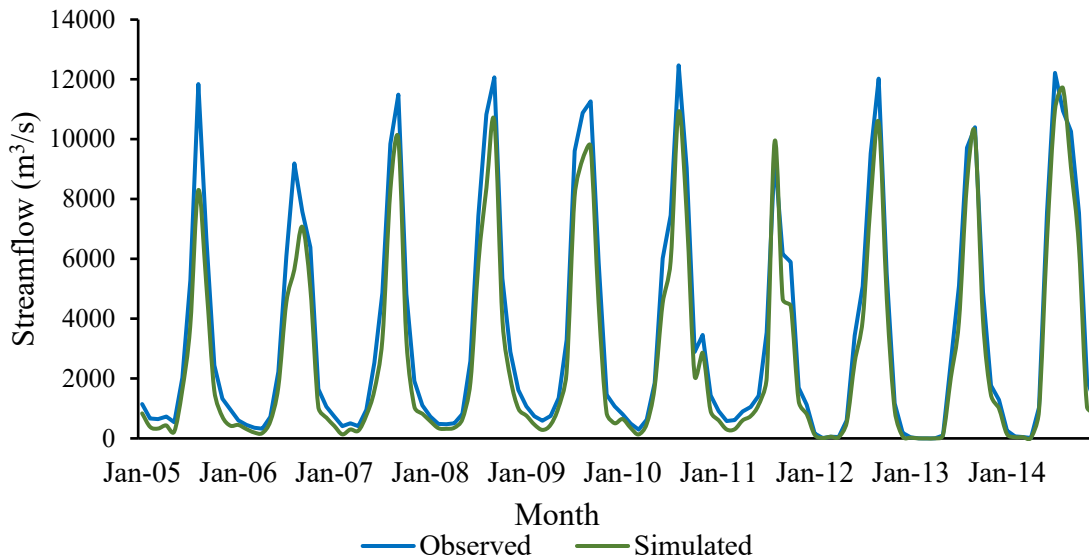


**Figure 6. Observed and simulated streamflow values for model validation (2005–2014)**

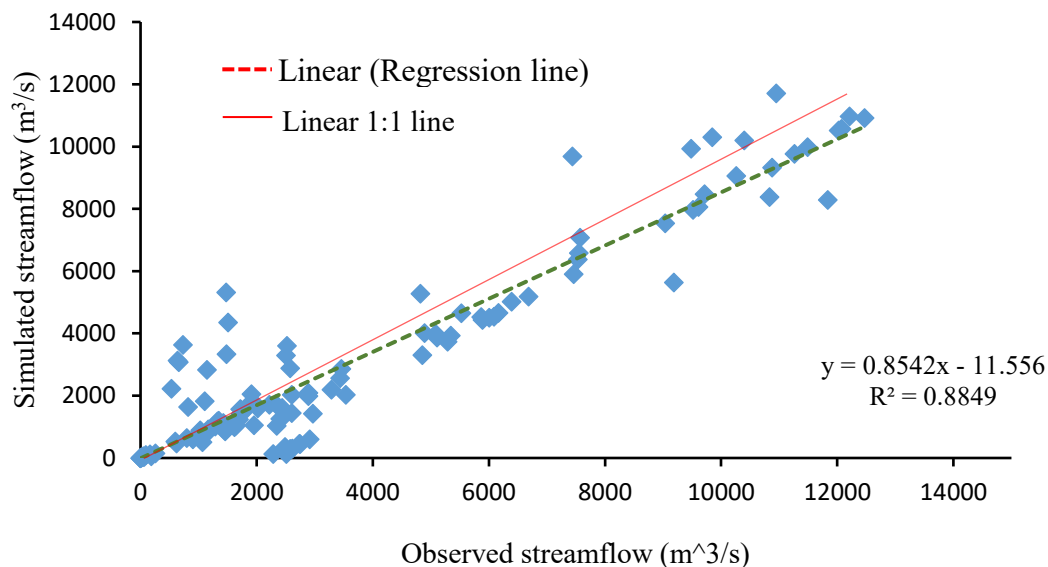


**Figure 7. Scatter plot depicting the comparison between observed and simulated streamflow during the validation period (2005–2014).**

### 3.4 Impacts of Climate and Land Use/Land Cover Variability on Hydrological Processes

The combined effects of climate variability and land use/land cover (LULC) changes on hydrological processes in the Upper Omo Gibe catchment were assessed using the MIKE SHE model over a three-decade period (1990–2020). This study aimed to investigate how these factors influence streamflow, subsurface flow, and evapotranspiration across different climatic and land use conditions (Table 8). By integrating observed climate data with LULC maps, the

model successfully captures long-term hydrological trends and the interactions between surface and subsurface water dynamics. These findings align with previous studies indicating that climate change and anthropogenic land use modifications significantly alter hydrological cycles, often leading to increased surface runoff, reduced groundwater recharge, and shifts in evapotranspiration patterns (Beven & Freer, 2001; Wagner & Gupta, 2005).

The results of this analysis demonstrate that streamflow generally increased in the later periods (SC3) due to reduced vegetation cover

and heightened surface runoff, while both subsurface flow and evapotranspiration showed a declining trend due to urbanization and reduced infiltration capacity (Chen et al., 2017). These patterns are consistent with the findings of Todini (2008), who emphasized that reductions in vegetation cover lead to increased direct runoff and decreased soil moisture retention, subsequently affecting base flow contributions to river systems. Furthermore, studies by Li et al. (2019) and Zhang et al. (2021) highlight that urbanization and deforestation exacerbate hydrological extremes, leading to more frequent

high-flow events and diminishing groundwater recharge rates.

This structured, scenario-based analysis offers valuable insights into the hydrological consequences of climate and land use changes, underscoring the importance of integrated watershed management strategies for the region. Effective land use planning and climate adaptation strategies, as suggested by Gupta et al. (2000) and Babovic & Bojkov (2001), are crucial in mitigating adverse hydrological impacts and ensuring sustainable water resource management in vulnerable basins such as the Upper Omo Gibe.

**Table 9. Mean annual hydrological components are assessed across varying land use classifications under different climatic conditions.**

Scenarios	Climate	Land use	Precipitation (mm/yr)	Streamflow (mm/yr)	Subsurface flow (mm/yr)	Evapotranspiration (mm/yr)
SC1	1990-2000	1990	1489.2	3475	425.0	130.0
SC1	2001-2010	1990	1590.8	3905	445.0	145.0
SC1	2011-2020	1990	1457.3	3920	400.0	120.0
SC2	1990-2000	2005	1489.2	3575	395.0	140.0
SC2	2001-2010	2005	1590.8	3975	375.0	138.0
SC2	2011-2020	2005	1457.3	4450	355.0	110.0
SC3	1990-2000	2020	1489.2	3825	300.0	100.0
SC3	2001-2010	2020	1590.8	3925	285.0	120.0
SC3	2011-2020	2020	1457.3	4625	275.0	100.0

### 3.5 Impact of climate change on streamflow

Climate change significantly influences streamflow dynamics by altering precipitation patterns, temperature regimes, and evapotranspiration rates. In the Upper Omo Gibe catchment, these climatic variations have led to substantial changes in surface runoff, subsurface flow, and overall hydrological responses over the past three decades. Using the MIKE SHE model, this study evaluates how fluctuations in climate drive changes in streamflow and related hydrological components under different land use conditions, providing valuable insights for water resource management and adaptation strategies. The analysis of mean annual precipitation and hydrological components under different climatic periods (1990–2000, 2001–2010, and 2011–2020) across scenarios SC1, SC2, and SC3 reveals distinct hydrological responses (Table 9). SC1, which represents the 1990 land use under different climate conditions, shows that an

increase in precipitation from 1489.2 mm to 1590.8 mm between the first and second periods results in a significant rise in streamflow (from 3475 mm to 3905 mm). However, a subsequent decrease in precipitation to 1457.3 mm (2011–2020) still leads to a rise in streamflow (3920 mm), suggesting that factors beyond precipitation, such as changes in infiltration rates and land use dynamics, may be influencing runoff processes. Additionally, subsurface flow follows a fluctuating trend, increasing from 425.0 mm to 445.0 mm before dropping to 400.0 mm in the final period, while evapotranspiration shows a similar decline, from 130.0 mm to 120.0 mm. These patterns align with previous studies indicating that climate-induced variations in hydrology are influenced not only by precipitation but also by shifts in land use and vegetation cover (Beven & Freer, 2001; Gupta et al., 2000).

In SC2, which represents the 2005 land use under the same climatic conditions, the results indicate that land cover changes alter hydrological responses. Streamflow increases from 3575 mm (1990–2000) to 3975 mm (2001–2010) and then rises sharply to 4450 mm (2011–2020), despite a decrease in precipitation in the final period. The decline in subsurface flow (from 395.0 mm to 355.0 mm) and evapotranspiration (from 140.0 mm to 110.0 mm) highlights a shift in hydrological partitioning, where more water contributes to surface runoff due to reduced infiltration capacity (Locatelli et al., 2017). This is consistent with findings by Todini (2008) and Zhang et al. (2021), who noted that land use changes, such as deforestation and urban expansion, tend to enhance surface runoff while reducing groundwater recharge.

SC3, representing the 2020 land use, exhibits the most pronounced changes, with streamflow increasing dramatically from 3825 mm (1990–2000) to 4625 mm (2011–2020), despite a slight decline in precipitation. The subsurface flow experiences a significant reduction, from 300.0 mm to 275.0 mm, while evapotranspiration continues to decline, reaching its lowest value of 100.0 mm in the most recent period. These results reinforce the argument that changes in land cover amplify the impacts of climate variability, as reduced vegetation cover and increased impervious surfaces lead to higher runoff and lower groundwater recharge (Li et al., 2019; Wagener & Gupta, 2005). The declining trend in evapotranspiration also suggests that reduced vegetation density and soil moisture availability are limiting atmospheric water loss, a pattern observed in studies on climate-induced changes in hydrology (Babovic & Bojkov, 2001).

The MIKE SHE model has proven effective in capturing these climate-driven hydrological changes, with model performance evaluations based on criteria established by Moriasi et al. (2007) confirming its ability to simulate watershed dynamics with high accuracy. The results of this study reinforce existing evidence on the interplay between climate change and hydrology, further supporting the necessity for proactive management strategies to mitigate climate-induced hydrological impacts (Gries et al., 2019). Given the increasing variability in

precipitation and temperature, integrating climate-resilient water management policies will be crucial for ensuring sustainable water resource availability in the Upper Omo Gibe catchment and beyond.

### **3.6 Impact of Climate and Land Use/Land Cover Changes on Hydrological Processes**

The combined and separate effects of climate variability and land use/land cover (LULC) changes significantly influence hydrological processes, altering surface runoff, subsurface flow, and evapotranspiration (ET) in the Upper Omo Gibe Basin. Figure 8 highlights the spatiotemporal impacts of these factors on hydrological components, showing distinct variations in surface runoff, subsurface flow, and ET across different periods.

#### **3.6.1 Variability in Surface Runoff**

Surface runoff exhibited a notable increase of 10.29% during 2001–2010, coinciding with an increase in mean annual precipitation from 1489.2 mm (1990–2000) to 1590.8 mm (2001–2010) (Figure 8a). However, the subsequent period (2011–2020) experienced a 2.38% decline in surface flow, as precipitation decreased to 1457.3 mm. This trend suggests that climate-driven changes in precipitation patterns directly influence streamflow generation, consistent with previous studies indicating that increased rainfall enhances direct runoff, while reduced precipitation limits water availability for surface flow (Beven & Freer, 2001; Todini, 2008).

In addition to climate variability, LULC changes played a crucial role in modifying runoff responses. Over the past three decades, agricultural expansion and deforestation have significantly altered infiltration capacities, leading to increased runoff generation. Studies by Derebe et al. (2022) and Lukas et al. (2023) confirm extensive agricultural expansion and significant losses in shrub land and forest cover, which reduce infiltration rates and exacerbate runoff generation. Similar findings in the Gilgel Gibe catchment, a sub-basin of the Upper Omo Gibe Basin, indicate that deforestation and land use modifications amplify peak flows and flood risks, intensifying regional water resource

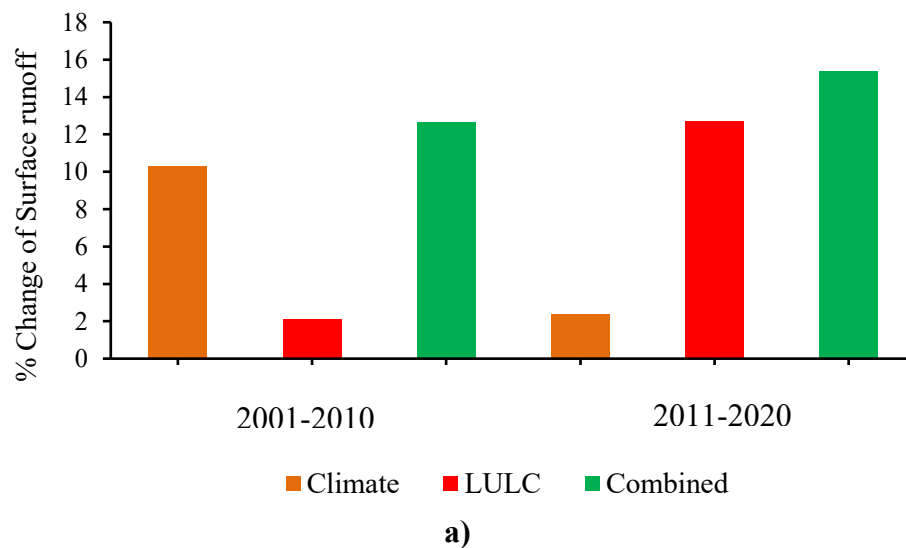
management challenges (Chaemiso et al., 2016; Orkodjo et al., 2022).

### 3.6.2 Changes in Subsurface Flow

Subsurface flow followed a similar trend, increasing by 7.43% during 2001–2010, reflecting enhanced groundwater recharge due to increased precipitation. However, a 10.39% decline in subsurface flow during 2011–2020 was observed, aligning with reduced precipitation and extensive land cover modifications (Figure 8b). The long-term decline in shrub land (-79.85%) and forest cover (-50.17%) (Table 5) has led to diminished infiltration rates, further reducing groundwater recharge. This pattern aligns with findings by Mekuria (2022) and Gebremichael et al. (2024), who reported that land cover changes in the basin, particularly deforestation and expansion of agricultural land, have significantly reduced groundwater contributions to streamflow.

### 3.6.3 Evapotranspiration Dynamics

Evapotranspiration (ET) experienced an increase of 10.03% during 2001–2010, corresponding to higher precipitation and improved vegetation water uptake. However, a 21.65% decrease in ET was recorded during 2011–2020, likely due to declining vegetation cover and soil moisture availability (Figure 8c). The substantial reductions in shrub land and forest cover (Table 5) contributed to lower ET rates, as vegetative transpiration plays a crucial role in regulating atmospheric moisture fluxes. Li et al. (2019) and Wagener & Gupta (2005) similarly reported that deforestation-driven reductions in ET result in decreased soil moisture retention and altered local climate conditions, further exacerbating hydrological changes.



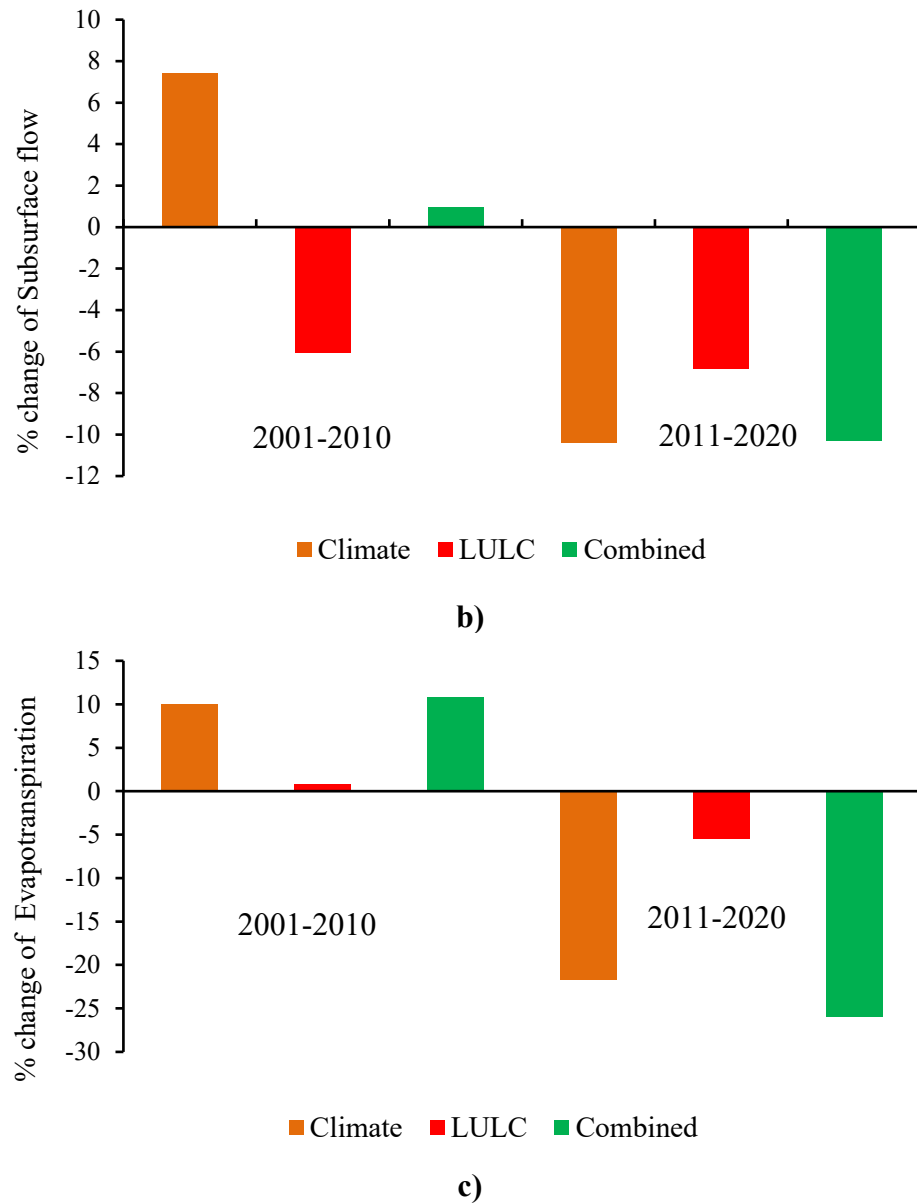


**Figure 8. The impacts of both separate and combined climate and LULC changes, a) Surface runoff; b) subsurface flow; c) evapotranspiration**

### 3.7 Impact of Land use change on streamflow

Land use and land cover (LULC) changes play a significant role in altering hydrological processes, affecting surface runoff, infiltration, evapotranspiration, and groundwater recharge. The analysis of various land use scenarios in Table 8 highlights how deforestation, agricultural expansion, and urbanization have transformed the hydrological dynamics of the Upper Omo Gibe catchment. The results indicate that these anthropogenic activities have led to substantial

modifications in streamflow, emphasizing the importance of sustainable land management in mitigating hydrological alterations.

### Hydrological Impacts of Land Use and Land Cover Changes on Streamflow and Runoff Dynamics

An analysis of land use and land cover (LULC) changes reveals a profound impact on the catchment's hydrological components across various periods. When compared to the 1990

baseline scenario (SC1), streamflow decreased by 4.72% in the 2005 scenario (SC4) and by 10.65% in the 2020 scenario (SC7). This corresponded with a long-term reduction in subsurface flow, which fell by 9.7 mm in 2005 and 40 mm in 2020. These findings underscore that LULC changes, driven primarily by deforestation and urbanization, are key factors in altering streamflow patterns.

During the periods from 2001–2010 and 2011–2020, a significant increase in surface runoff was observed, rising by 2.14% and 12.72%, respectively. In contrast, subsurface flow declined by 6.03% and 6.82%, while evapotranspiration decreased by 0.75% and 5.49% (Figures 8a and 8b). The expansion of agricultural and settlement areas has been the primary driver of this trend. A LULC analysis showed that between 1990 and 2020, agricultural land expanded by 27.73% and settlement areas grew by an alarming 81.0%. As natural vegetation, such as forests and shrub lands, was converted to croplands and urban areas, the land's capacity to retain and absorb rainfall diminished. This transformation has shifted the catchment's hydrological response, resulting in increased peak flows, reduced groundwater recharge, and higher flood risks.

The observations are consistent with a growing body of research showing that the expansion of agricultural and settlement areas leads to increased impervious surfaces, which in turn reduces soil infiltration and exacerbates surface runoff (Kim et al., 2002; Dibaba et al., 2020; Kumar et al., 2022). Furthermore, the reduction of natural water bodies, forests, and shrub lands contributes to a decline in subsurface flow and evapotranspiration, thereby fundamentally altering the catchment's overall water balance (Mekonnen et al., 2018; Malede et al., 2023).

### 3.8 Combined Impacts of Climate and Land Use Change

The combined effects of climate change and land use/land cover (LULC) alterations on runoff dynamics, water resource availability, and ecosystem resilience highlight the intricate interactions between these two factors (Gelfan et al., 2017). Climate variability and land use modifications significantly influence

hydrological components, affecting surface runoff, subsurface flow, and evapotranspiration patterns. By integrating climate data from 1990 to 2020 with corresponding LULC maps, the study examined the interplay between these drivers and their collective impact on streamflow within the Upper Omo Gibe Basin.

### Hydrological Responses to Climate and Land Use Interactions

The findings indicate that during 2001–2010 (SC1 to SC2), surface flow increased by 446.5 mm, corresponding with a 101.6 mm rise in precipitation, a 3.7 mm increment in subsurface flow, and a 13.3 mm increase in evapotranspiration. However, from 2011–2020 (SC2 to SC3), while streamflow further increased by 605.3 mm, precipitation declined by 133.5 mm, subsurface flow decreased by 100.2 mm, and evapotranspiration dropped by 39.8 mm. These results suggest that although precipitation initially supported increased runoff and evapotranspiration, the subsequent reduction in precipitation combined with LULC changes led to a marked shift in hydrological components, notably decreasing subsurface flow and evapotranspiration.

The absence of a linear trend in runoff responses across the scenarios highlights the complex interplay between climate variability and LULC changes (Nigusie & Dananto, 2021). While the overall effect resulted in increased streamflow, the magnitude and direction of changes in subsurface flow and evapotranspiration varied. The increasing surface runoff (12.63% from 2001–2010 and 15.40% from 2011–2020) and declining subsurface flow (ranging from -0.94% to -10.30%) reinforce the notion that deforestation, urban expansion, and declining precipitation jointly contribute to increased surface runoff and reduced groundwater recharge.

### 3.9 Runoff to Rainfall Ratio and Dryness Index

The runoff-to-rainfall ratio (RR) and the dryness index (ET/P) provide key insights into how climatic and land cover transformations shape hydrological balance (Figure 9). The analysis indicates that from 1990–2000 to 2011–2020, the

RR increased by 34%, while ET/P declined by 1.6%, reflecting reduced moisture availability and higher runoff generation. Over this period, precipitation declined by 2.14%, yet runoff increased by 12.8%, and evapotranspiration dropped by 24.62%. These findings confirm that land use shifts, particularly deforestation and expansion of agricultural and settlement areas, exacerbated surface runoff while reducing

evapotranspiration and infiltration. Similar trends have been documented in prior studies, indicating the dominant role of LULC changes in modifying runoff ratios and evapotranspiration balances (Mengistu & Sorteberg, 2012; Gebremicael *et al.*, 2017; Kumar *et al.*, 2022; Malede *et al.*, 2023).

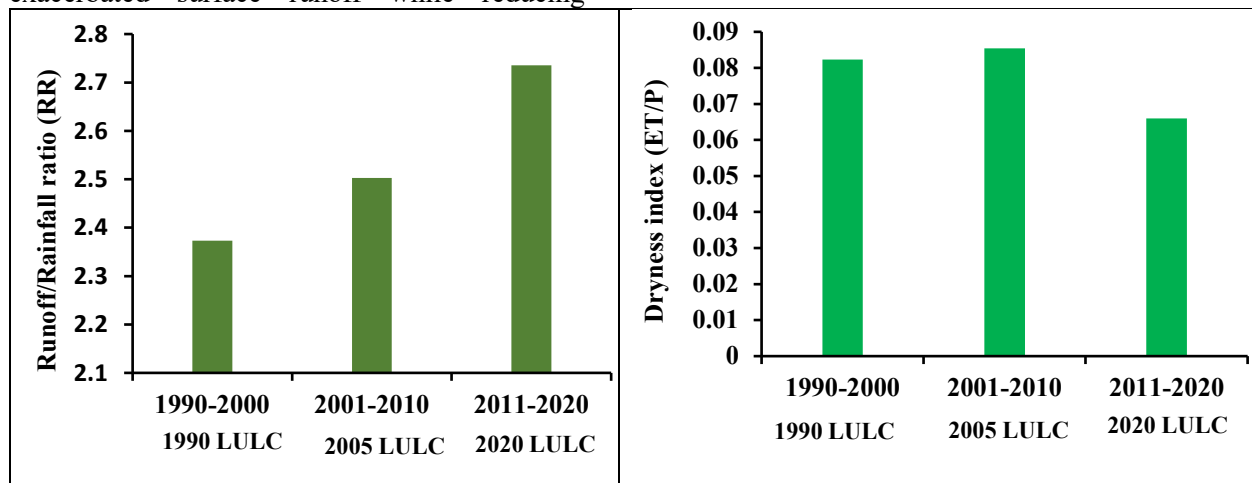


Figure 9. Ratios of runoff to rainfall (RR) and the dryness index (ET/P) analyzed for the period 1990 – 2020.

### 3.10 Implications for Water Resource Management

The Upper Omo Gibe Basin's hydrological processes are significantly altered by climate and LULC changes, evidenced by increased surface runoff, reduced subsurface flow/ET, and disrupted water cycling. MIKE SHE model simulations (validated via Moriasi *et al.*, 2007 criteria) highlight risks like groundwater depletion, soil erosion, and flash floods. Adaptive strategies (e.g., afforestation, sustainable land use, soil conservation) are critical to mitigate impacts, aligning with findings by Chaemiso *et al.* (2016), Mekuria (2022), and Orkodjo *et al.* (2022). Integration of hydrological models into land-use planning and policy frameworks is urged to enhance climate resilience and water sustainability. Collaborative efforts among policymakers, researchers, and communities are essential for balancing basin hydrology amid ongoing environmental changes.

### 4. Conclusions

The impact of climate and land use/land cover (LULC) changes on streamflow in the Upper Omo Gibe Basin has resulted in significant shifts in hydrological patterns. The expansion of agricultural and urban areas has reduced soil infiltration and increased surface runoff, leading to more frequent and severe flooding events. In contrast, the reduction of forest and shrub land areas has diminished subsurface flow and evapotranspiration rates, disrupted the hydrological balance and negatively affected groundwater recharge.

Further complicating the situation, climate change has altered precipitation and temperature patterns, influencing streamflow volumes. This demonstrates the intricate interplay between natural processes and human activities in shaping hydrological dynamics. Analyses of the 2001–2010 and 2011–2020 periods revealed contrasting trends in surface and subsurface flows, underscoring the need for adaptive water management strategies. The MIKE SHE model effectively simulated hydrological processes in



the catchment, with calibration and validation yielding NSE and  $R^2$  values exceeding 0.80. Surface runoff has increased by 2.14% and 12.72% in the respective decades, while subsurface flow decreased by 6.03% and 6.82%, and evapotranspiration dropped by 0.75% and 5.49%. These changes reflect more substantial collective effects than individual impacts, driving significant hydrological shifts in the region. Notably, while subsurface flow and evapotranspiration increased during 2001–2010, they declined in the 2011–2020 period, signaling a negative trend in overall hydrological balance. To mitigate the adverse effects of increased surface runoff and decreased subsurface flow, it is crucial to prioritize sustainable land use practices. These include afforestation, agroforestry, and the conservation of natural vegetation, which can enhance infiltration, reduce surface runoff, and support groundwater recharge. Furthermore, investing in climate-resilient infrastructure, such as flood control systems and rainwater harvesting, will help manage runoff and minimize flood risks. The implementation of Integrated Water Resource Management (IWRM) strategies is essential for adaptive water management, considering the combined impacts of climate and LULC changes on hydrological dynamics. Ongoing monitoring and modeling with tools like MIKE SHE will aid in making accurate predictions and informed decisions under varying conditions. Engaging local communities in sustainable land and water practices will foster resilience, contributing to long-term environmental sustainability in the watershed and ensuring that future generations can effectively manage the region's water resources.

### Modeling Limitations and Future Considerations

While the study provided valuable insights, certain limitations should guide future research. The model's accuracy is heavily dependent on reliable, long-term climate and hydrological datasets. The computational demands of the MIKE SHE model, particularly for fine-scale analysis, also present a constraint on extensive simulations. Future efforts should therefore focus on enhancing data collection, refining model

calibration processes, and incorporating more detailed representations of LULC changes to better capture hydrological responses.

Based on these findings, several directions are recommended for future research. Expanding the temporal scope to include future climate scenarios would allow for long-term hydrological trend projections, providing crucial information for proactive water management. Furthermore, future studies should incorporate socioeconomic factors by linking LULC changes to demographic and economic drivers, such as population growth and agricultural policies, to gain more holistic insights for governance. Finally, fostering interdisciplinary collaboration with ecologists and policymakers is essential to co-design effective and adaptive strategies, such as payment for ecosystem services, that can sustainably manage the catchment's water resources.

### Author Contributions:

Kindie Zewdie Werede: Conceptualization, software/statistical analysis, writing the initial version of the article

Tarun Kumar Lohani: Guidance, editing, and reviewing the article, controlling the results

Bogale Gebremariam Neka: Conceptualization, consulting, reviewing the text of the article, and statistical analysis

Getachew Bereta Geremew: Reviewing the text of the article, statistical analysis

### Conflicts of interest

The authors of this article declared no conflict of interest regarding the authorship or publication of this article.

### Data availability statement:

All data generated or analyzed during this study are included in this published article.

### References

Abate, A., Mulat, W. L., & Mekonnen, M. M. (2025). Optimizing Water Resources Allocation in the Nile Basin: Analyzing Long-Term Changes in Water Footprint and Virtual Water Trade for Sustainability. *Ethiopian Economics Association (EEA)*, 29.

- Abbott, M. B., et al. (1986). "An introduction to the European Hydrological System—Systeme Hydrologique Europeen, 'SHE', 1: History and philosophy of a physically-based, distributed modelling system." *Journal of Hydrology*, 87(1), 45-59. doi: 10.1016/0022-1694(86)90114-9
- Allen, R. G., Pereira, L. S., Raes, D., & Smith, M. (1998). Crop evapotranspiration—Guidelines for computing crop water requirements—FAO Irrigation and drainage paper 56. FAO. <https://www.fao.org/3/x0490e/x0490e00.htm>
- Anderson, J. R. (1976). *A land use and land cover classification system for use with remote sensor data* (Vol. 964). US Government Printing Office. doi: 10.3133/pp964
- Aredo, M. R., Hatiye, S. D., & Pingale, S. M. (2021). Impact of land use/land cover change on stream flow in the Shaya catchment of Ethiopia using the MIKE SHE model. *Arabian Journal of Geosciences*, 14(2), 1–15. doi: 10.1007/s12517-021-06447-2
- Aredo, M. R., Hatiye, S. D., & Pingale, S. M. (2021). Modeling the rainfall-runoff using MIKE 11 NAM model in Shaya catchment, Ethiopia. *Modeling Earth Systems and Environment*, 7(4), 2545-2551. doi: 10.1007/s40808-020-01054-8
- Ayana, E. K., Edossa, D. C., & Mengistu, D. T. (2021). Evaluating the impacts of land use land cover and climate change on streamflow in Gilgel Gibe watershed, Ethiopia, using MIKE SHE hydrological model. *Sustainable Water Resources Management*, 7(4), 1–12. doi: 10.1007/s40899-021-00560-6
- Awulachew, S. B., Yilma, A. D., Loulseged, M., Loiskandl, W., Ayana, M., & Alamirew, T. (2007). *Water resources and irrigation development in Ethiopia* (Vol. 123). IWMI.
- Babovic, V., & Bojkov, V. H. (2001). Runoff modeling with genetic programming and artificial neural networks. D2K Technical Report 0401-1. Danish Hydraulics Institute, Denmark.
- Beck, H. E., Zimmermann, N. E., McVicar, T. R., Vergopolan, N., Berg, A., & Wood, E. F. (2018). Present and future Köppen-Geiger climate classification maps at 1-km resolution. *Scientific Data*, 5, 180214. doi: 10.1038/sdata.2018.214
- Belay, T., & Mengistu, D. A. (2021). *Impacts of land use/land cover and climate changes on soil erosion in Muga watershed, Upper Blue Nile basin (Abay), Ethiopia. Ecol. Process.* 10 (1), 1–21 (p. 68). doi: 10.1186/s13717-021-00339-9
- Berhanu, B., Seleshi, Y., & Melesse, A. M. (2013). GIS-based hydrological zones and soil geo-database of Ethiopia. *Catena*, 104, 21–31. doi: 10.1016/j.catena.2012.12.007
- Butts, M. B., et al. (2004). "An evaluation of the performance of catchment-scale models." *Journal of Hydrology*, 293(1-4), 256-279. doi: 10.1016/j.jhydrol.2004.01.010
- Beven, K. J., & Freer, J. (2001). Equifinality, data assimilation, and uncertainty estimation in mechanistic modelling of complex environmental systems using the GLUE methodology. *Journal of Hydrology*, 249(1–4), 11–29. doi: 10.1016/S0022-1694(01)00421-8
- Chaemiso, S. E., Abebe, A., & Pingale, S. M. (2016). Assessment of the impact of climate change on surface hydrological processes using SWAT: a case study of Omo-Gibe river basin, Ethiopia. *Modeling Earth Systems and Environment*, 2(4), 1–15. doi: 10.1007/s40808-016-0257-9
- Chen, J., Theller, L., Gitau, M. W., Engel, B. A., & Harbor, J. M. (2017). Urbanization impacts on surface runoff of the contiguous United States. *Journal of Environmental Management*, 187, 470–481. doi: 10.1016/j.jenvman.2016.11.017.
- Congalton, R. G., & Green, K. (2019). *Assessing the accuracy of remotely sensed data: principles and practices*. CRC press. doi: 10.1201/9781420055139
- Degefu, M. A., & Bewket, W. (2014). Variability and trends in rainfall amount and extreme event indices in the Omo-Ghibe River Basin, Ethiopia. *Regional environmental change*, 14(2), 799-810. doi: 10.1007/s10113-013-0538-z
- Derebe, M. A., Hatiye, S. D., & Asres, L. A. (2022). Dynamics and Prediction of Land Use and Land Cover Changes Using Geospatial Techniques in Abelti Watershed, Omo Gibe River Basin, Ethiopia. *Advances in*

- Agriculture*, 10, 1–9. doi: 10.1155/2022/1862461
- DHI. (2023). "MIKE SHE – Integrated Catchment Modeling." DHI Group. Link
- Elias, E. (2017). Characteristics of Nitisols: *Soils of the Ethiopian Highlands*. Soil Atlas of Africa, Ethiopia Ministry of Agriculture and Natural Resources, pp. 132–133. doi: 10.5281/zenodo.2553416
- FAO (2001). Food and Agriculture Organization of the United Nations Viale delle Terme di Caracalla, 00100 Rome, Italy. ISBN 92-5-104628-X
- Foody, G. M. (2002). Status of land cover classification accuracy assessment. *Remote Sensing of Environment*, 80(2), 185–201. doi: 10.1016/S0034-4257(01)00295-4
- Gebrehiwot, S. G., Taye, M. T., & Bishop, K. (2022). Integrated water resources management under climate change in the Upper Blue Nile Basin, Ethiopia. *Journal of Hydrology: Regional Studies*, 40, 100982. doi: 10.1016/j.ejrh.2022.100982
- Gebremicael, T. G., Mohamed, Y. A., & Hagos, E. Y. (2017). Temporal and spatial changes of rainfall and streamflow in the Upper Tekezē–Atbara river basin, Ethiopia. *Hydrology and Earth System Sciences*, 21(4), 2127–2142. doi: 10.5194/hess-21-2127-2017
- Gebremichael, A., Kebede, A., & Woyessa, Y. E. (2024). Impact of climate change on water resource potential and sediment yield of the Gibe III watershed, Omo-Gibe Basin, Ethiopia. *Journal of Water and Climate Change*, 15(3), 902–920. doi: 10.2166/wcc.2024.292
- Gelfan, A., Motovilov, Y., & Gustafsson, D. (2017). Testing the robustness of the physically-based ECOMAG model with respect to changing conditions. *Hydrological Sciences Journal*, 62(1), 40–54. doi: 10.1080/02626667.2014.967694
- Getachew, B., Manjunatha, B. R., & Bhat, H. G. (2021). Modeling projected impacts of climate and land use/land cover changes on hydrological responses in the Lake Tana Basin, upper Blue Nile River Basin, Ethiopia. *Journal of Hydrology*, 595, 125974.
- Gisha Kuma, H., Mekonnen Chinasho, E., & Asha Tolke, A. (2024). Evaluation of hydrological responses to climate change in the Gibe Gojeb catchment, southwestern Ethiopia. *Journal of Water and Climate Change*, 15(5), 2232–2243. doi: 10.2166/wcc.2024.656
- Gitima, G., Teshome, M., Kassie, M., & Jakubus, M. (2023). Quantifying the impacts of spatiotemporal land use and land cover changes on soil loss across agroecologies and slope categories using GIS and RUSLE model in Zoa watershed, southwest Ethiopia. *Ecological Processes*, 12(1), 24.
- Graham, D. N., & Butts, M. B. (2005). "Flexible, integrated watershed modelling with MIKE SHE." In *Watershed Models* (pp. 245–272). CRC Press.
- Gries, T., Redlin, M., & Ugarte, J. E. (2019). Human-induced climate change: the impact of land-use change. *Theoretical and Applied Climatology*, 135(15), 1031–1044. doi: 10.1007/s00704-018-2422-8
- Guduru, J. U., Jilo, N. B., Rabba, Z. A., & Namara, W. G. (2023). Rainfall-runoff modeling using HEC-HMS model for Meki River watershed, rift valley basin, Ethiopia. *Journal of African Earth Sciences*, 197, 104743. doi: 10.1016/j.jafrearsci.2022.104743
- Gupta, A. K., & Govindarajan, V. (2000). Knowledge flows within multinational corporations. *Strategic Management Journal*, 21(4), 473–496. doi: 10.1002/(SICI)1097-0266(200004)21:4<473::AID-SMJ84>3.0.CO;2-I
- Gupta, H. V., et al. (2009). "Decomposition of the mean squared error and NSE performance criteria: Implications for improving hydrological modelling." *Journal of Hydrology*, 377(1-2), 80–91. doi: 10.1016/j.jhydrol.2009.08.003
- Guzha, A. C., Rufino, M. C., Okoth, S., Jacobs, S., & Nóbrega, R. L. B. (2018). Impacts of land use and land cover change on surface runoff, discharge and low flows: Evidence from East Africa. *Journal of Hydrology: Regional Studies*, 15, 49–67. doi: 10.1016/j.ejrh.2017.11.005
- Haddeland, I., Heinke, J., Biemans, H., Eisner, S., Flörke, M., Hanasaki, N., Konzmann, M., Ludwig, F., Masaki, Y., Schewe, J., Stacke, T., Tessler, Z. D., Wada, Y., & Wisser, D. (2014).

- Global water resources affected by human interventions and climate change. *Proceedings of the National Academy of Sciences*, 111(9), 3251–3256. doi: 10.1073/pnas.1222475110
- Han, Q., Xue, L., Qi, T., Liu, Y., Yang, M., Chu, X., & Liu, S. (2023). Assessing the Impacts of Future Climate and Land-Use Changes on Streamflow under Multiple Scenarios: A Case Study of the Upper Reaches of the Tarim River in Northwest China. *Water*, 16(1), 100. doi: 10.3390/w16010100
- Hussen, A. A., Birhanu, B. S., & Melesse, A. M. (2021). Hydrological impacts of climate change on the Upper Blue Nile River Basin, Ethiopia. *Hydrology*, 8(1), 12. doi: 10.3390/hydrology8010012
- Ismail, M. H., & Jusoff, K. (2008). Satellite data classification accuracy assessment based from reference dataset. *World Academy of Science, Engineering and Technology. International Journal of Geological and Environmental Engineering*, 2(3), 23–29.
- Kasei, C. N., Diekkrüger, B., & Leemhuis, C. (2010). Drought frequency in the Volta Basin of West Africa. *Sustainability*, 2(7), 2175–2196. doi: 10.3390/su2072175
- Kumar, M., Denis, D. M., Kundu, A., Joshi, N., & Suryavanshi, S. (2022). Understanding land use/land cover and climate change impacts on hydrological components of Usri watershed, India. *Applied Water Science*, 12(3), 1–14. doi: 10.1007/s13201-021-01547-6
- Legates, D. R., & McCabe, G. J. (1999). "Evaluating the use of 'goodness-of-fit' measures in hydrologic and hydroclimatic model validation." *Water Resources Research*, 35(1), 233–241. doi: 10.1029/1998WR900018
- Li, S., Zhao, W. X., Yin, E. J., & Wen, J.-R. (2019). A neural citation count prediction model based on peer review text. In *Proceedings of the 2019 Conference on Empirical Methods in Natural Language Processing and the 9th International Joint Conference on Natural Language Processing (EMNLP-IJCNLP)* (pp. 4914–4924). Association for Computational Linguistics. doi: 10.18653/v1/D19-1497
- Locatelli, L., Mark, O., Mikkelsen, P. S., Arnbjerg-Nielsen, K., Deletic, A., Roldin, M., & Binning, P. J. (2017). Hydrologic impact of urbanization with extensive stormwater infiltration. *Journal of Hydrology*, 544, 524–537. doi: 10.1016/j.jhydrol.2016.11.030
- Loliyana, V. D., & Patel, P. L. (2018). Performance evaluation and parameters sensitivity of a distributed hydrological model for a semi-arid catchment in India. *Journal of Earth System Science*, 127(117), 1–26. doi: 10.1007/s12040-018-1021-5
- Lu, D., & Weng, Q. (2007). A survey of image classification methods and techniques for improving classification performance. *International Journal of Remote Sensing*, 28(5), 823–870. doi: 10.1080/01431160600746456
- Lucas-Borja, M. E., Carrà, B. G., Nunes, J. P., Bernard-Jannin, L., Zema, D. A., & Zimbone, S. M. (2020). Impacts of land-use and climate changes on surface runoff in a tropical forest watershed (Brazil). *Hydrological Sciences Journal*, 65(11), 1956–1973. doi: 10.1080/02626667.2020.1787417
- Lukas, P., Melesse, A. M., & Kenea, T. T. (2023). Prediction of future land use/land cover changes using a coupled CA-ANN model in the upper omo-gibe river basin, Ethiopia. *Remote Sensing*, 15(4), 1148. doi: 10.3390/rs15041148
- Malede, D. A., Alamirew, T., & Andualem, T. G. (2023). Integrated and Individual Impacts of Land Use Land Cover and Climate Changes on Hydrological Flows over Birr River Watershed, Abbay Basin, Ethiopia. *Water (Switzerland)*, 15(1). doi: 10.3390/w15010166
- Mekuria, E. T. (2022). Assessment of Water Balance of Deme Watershed, Omo-Gibe Basin, Ethiopia Using SWAT Model and ARC-GIS for Water Resources Management. *Journal of Water Resources and Ocean Science*, 11(6), 86–98.
- Mekuria, E. T. (2022). Assessment of spatial soil erosion using RUSLE model integration with GIS and RS tools a case study of Gojeb catchment, Omo-Gibe Basin, Ethiopia. *International Journal of Environmental Protection and Policy*, 10(5), 130–139. doi: 10.11648/j.ijepp.20221005.13

- Mengistu, D. T., & Sorteberg, A. (2012). Sensitivity of SWAT simulated streamflow to climatic changes within the Eastern Nile River basin. *Hydrology and Earth System Sciences*, 16(2), 391–407. doi: 10.5194/hess-16-391-2012
- Milly, P. C. D., Dunne, K. A., & Vecchia, A. V. (2005). "Global pattern of trends in streamflow and water availability in a changing climate." *Nature*, 438(7066), 347–350. doi: 10.1038/nature04312
- Moriasi, D. N., Arnold, J. G., Van Liew, M. W., Bingner, R. L., Harmel, R. D., & Veith, T. L. (2007). Model evaluation guidelines for systematic quantification of accuracy in watershed simulations. *Transactions of the ASABE*, 50(3), 885–900. doi: 10.13031/2013.23153
- Nath, S. S., Mishra, G., Kar, J., Chakraborty, S., & Dey, N. (2014). A survey of image classification methods and techniques. *2014 International Conference on Control, Instrumentation, Communication and Computational Technologies (ICCICCT)*, 554–557.
- Nigusie, A., & Dananto, M. (2021). Impact of land use/land cover change on hydrologic processes in Dijo watershed, central rift valley, Ethiopia. *International Journal of Water Resources and Environmental Engineering*, 13(1), 37–48. doi: 10.5897/IJWREE2020.0956
- Orkodjo, T. P., Kranjac-Berisavijevic, G., & Abagale, F. K. (2022). Impact of climate change on future precipitation amounts, seasonal distribution, and streamflow in the Omo-Gibe basin, Ethiopia. *Heliyon*, 8(6), e09711. doi: 10.1016/j.heliyon.2022.e09711
- Ortiz, D. I., Piche-Ovares, M., Romero-Vega, L. M., Wagman, J., & Troyo, A. (2021). The impact of deforestation, urbanization, and changing land use patterns on the ecology of mosquito and tick-borne diseases in Central America. *Insects*, 13(1), 20. doi: 10.3390/insects13010020
- Paudel, S., & Benjankar, R. (2022). Integrated hydrological modeling to analyze the effects of precipitation on surface water and groundwater hydrologic processes in a small watershed. *Hydrology*, 9(2), 37. doi: 10.3390/hydrology9020037
- Sahoo, G. B., Ray, C., & De Carlo, E. H. (2006b). Use of neural network to predict flash flood and attendant water qualities of a mountainous stream on Oahu, Hawaii. *Journal of Hydrology*, 327(3–4), 525–538. doi: 10.1016/j.jhydrol.2005.11.059
- Shang, X., Jiang, X., & Jia, R. (2019). *Land Use and Climate Change Effects on Surface Runoff Variations in the Upper Heihe River Basin*. doi: 10.3390/w11020344
- Singh, V. P., & Woolhiser, D. A. (2002). "Mathematical modeling of watershed hydrology." *Journal of Hydrologic Engineering*, 7(4), 270–292. doi: 10.1061/(ASCE)1084-0699(2002)7:4(270)
- Talib, A., & Randhir, T. O. (2017). Climate change and land use impacts on hydrologic processes of watershed systems. *Journal of Water and Climate Change*, 8(3), 363–374. doi: 10.2166/wcc.2017.064
- Tarekegn, M. M., Uhlenbrook, S., Wenninger, J., & Savenije, H. H. (2021). Investigating the responses of hydrological processes to land use/cover changes in an Ethiopian river basin using a distributed hydrological model. *Water*, 13(1), 101. doi: 10.3390/w13010101
- Tassew, B. G., Belete, M. A., & Miegel, K. (2019). Application of HEC-HMS model for flow simulation in the Lake Tana basin: The case of Gilgel Abay catchment, upper Blue Nile basin, Ethiopia. *Hydrology*, 6(1), 21. doi: 10.3390/hydrology6010021
- Taye, M. T., Dyer, E., Hirpa, F. A., & Charles, K. (2018). Climate change impact on water resources in the Awash basin, Ethiopia. *Water*, 10(11), 1560. doi: 10.3390/w10111560
- Teshome, A., & Zhang, J. (2019). The role of hydropower in the economic development of Ethiopia and the implications for Nile river basin. *Renewable and Sustainable Energy Reviews*, 114, 109299. doi: 10.1016/j.rser.2019.109299
- Todini, E. (2008). A model conditional processor to assess predictive uncertainty in flood forecasting. *International Journal of River Basin Management*, 6(2), 123–137. doi: 10.1080/15715124.2008.9635342

- Truneh, A., Gebremichael, M., & Ayana, A. (2023). Impact of climate variability and land use/land cover changes on hydrological processes in the Rift Valley Lakes Basin, Ethiopia. *Water Resources Management*, 37(1), 381–397. doi: 10.1007/s11269-022-03359-5
- Vázquez, R. F., Feyen, L., Feyen, J., & Refsgaard, J. C. (2002). Effect of grid size on effective parameters and model performance of the MIKE-SHE code. *Hydrological Processes*, 16(2), 355–372. doi: 10.1002/hyp.334
- Wagner, T., & Gupta, H. V. (2005). Model identification for hydrological forecasting under uncertainty. *Stochastic Environmental Research and Risk Assessment*, 19(6), 378–387. doi: 10.1007/s00477-005-0006-5
- Werede, K. Z., Lohani, T. K., Neka, B. G., & Geremew, G. B. (2024). Modeling streamflow responses to land use and land cover change using MIKE SHE model in the upper Omo Gibe catchment of Ethiopia. *World Water Policy*, 10(3), 986–1009. doi: 10.1002/wwp2.12186
- Woldesenbet, T. A., Elagib, N. A., Ribbe, L., & Heinrich, J. (2020). Hydrological responses to land use/land cover change in the Upper Blue Nile Basin, Ethiopia. *Science of the Total Environment*, 742, 140504. doi: 10.1016/j.scitotenv.2020.140504
- World Meteorological Organization (WMO). (2008). "Guide to Hydrological Practices: Volume I, Hydrology – From Measurement to Hydrological Information." *WMO-No. 168*.
- Xia, Y., Koster, R. D., & Huang, M. (2020). Evaluation of monthly root-zone soil moisture from satellite observations and modeling: Implications for drought monitoring in the U.S. Great Plains. *Journal of Hydrometeorology*, 21(1), 5–23. doi: 10.1175/JHM-D-19-0115.1
- Yin, J., He, F., Jiu Xiong, Y., & Yu Qiu, G. (2017). Effects of land use/land cover and climate changes on surface runoff in a semi-humid and semi-arid transition zone in northwest China. *Hydrology and Earth System Sciences*, 21(1), 183–196. doi: 10.5194/hess-21-183-2017
- Zhang, Q., Li, J., Singh, V. P., & Xiao, M. (2013). Spatio-temporal relations between temperature and precipitation regimes: Implications for temperature-induced changes in the hydrological cycle. *Global and Planetary Change*, 111, 57–76. doi: 10.1016/j.gloplacha.2013.08.012
- Zhang, Z., Wang, S., Sun, G., McNulty, S. G., Zhang, H., Li, J., Zhang, M., Klaghofer, E., & Strauss, P. (2008). Evaluation of the MIKE SHE model for application in the Loess Plateau, China 1. *JAWRA Journal of the American Water Resources Association*, 44(5), 1108–1120. doi: 10.1111/j.1752-1688.2008.00244.x
- Zhang, R., Pang, C., Zhang, C., Wang, S., He, Z., Sun, Y., Wu, H., & Wang, H. (2021). Correcting Chinese spelling errors with phonetic pre-training. In Findings of the Association for Computational Linguistics: ACL-IJCNLP 2021 (pp. 2250–2261). Association for Computational Linguistics. doi: 10.18653/v1/2021.findings-acl.198